UNIVERSITY OF TURKU

Chemical synthesis and mass spectrometric detection of microbiome-derived N-acyl amides

Master's thesis
University of Turku
Department of Life Technologies
Molecular Systems Biology
May 2026

Melissa Ahonen

Master's thesis

Subject: Molecular Systems Biology
Author: Melissa Ahonen
Title: Chemical synthesis and mass spectrometric detection of microbiome-derived N-acyl amides
Supervisor: Professor Matej Orešič
Number of pages: 67 pages
Date: 10.5.2026

N-acyl amides (NAAs) are a structurally and functionally diverse group of endogenous cell signalling molecules, known for regulating several physiological responses in the body. Resent research has accumulated evidence for gut microbiome-derived NAAs that could influence the host physiology via gut-brain signalling. In the field of metabolomics, liquid chromatography-mass spectrometry represents the most extensively utilized analysis method. However, it has not been as widely applied in faecal analysis, which is the optimal biological sample matrix when investigating gut microbiome-derived metabolites, such as NAAs. The aims of this thesis were to chemically synthesize two NAA standards, histamine-C5:0 and Arg-C18:0, and to detect NAAs from human faecal samples using targeted mass spectrometric analysis.

Successful synthesis of histamine-C5:0 and Arg-C18:0 was confirmed with liquid chromatography-tandem mass spectrometry (LC-MS/MS) and nuclear magnetic resonance spectroscopy. The newly synthesized NAAs together with NAA standard mixtures provided by a collaborator were used as qualitative standards in faecal analysis. NAA profiling was conducted using a newly developed targeted LC-MS/MS method, with high selectivity based on retention time as well as predefined precursor ion and fragment ion spectrum matching.

In this study 32 NAAs were identified in human faecal samples with targeted LC-MS/MS. While there were no statistically significant differences in the relative abundances of NAAs between the sexes, these results demonstrated the utility of synthetic NAA standards together with optimized targeted LC-MS/MS method in detection of microbiome-derived NAAs in faecal samples, which have remained underexplored due to their biological complexity.

Key words: chemical synthesis, gut microbiome, liquid chromatography, mass spectrometry, N-acyl amides, nuclear magnetic resonance spectroscopy

Table of contents

1 Introduction

1.1 N-acyl amides

N-acyl amides (NAAs) are a group of endogenous cell signalling molecules that regulate numerous physiological responses in the body, particularly in the brain and central nervous system (CNS) (Waluk et al., 2014). This group consists of structurally and functionally diverse compounds that can bind to different receptors and, as a result, induce different biological responses.

Endocannabinoid system (ECS) is a neuro- and immunomodulator system that has an important role in maintaining the immune system homeostasis (Osafo et al., 2021). The ECS is comprised of endogenous signalling molecules, endocannabinoids, their receptors and enzymes involved in the pathways. Endocannabinoids have two main cell surface proteins that they interact with, cannabinoid receptor 1 (CB1) and cannabinoid receptor 2 (CB2), which are G-protein coupled receptors (GPCRs) (Devane et al., 1988; Iannotti et al., 2016; Munro et al., 1993; Osafo et al., 2021). The classical endocannabinoids that bind to these receptors are 2-arachidonyl-glyserol (2-AG) and N-arachidonoyl ethanolamine (AEA) (Iannotti et al., 2016). However, other endocannabinoid-related lipid mediators, such as NAAs, have been discovered that induce cannabimimetic effects. These compounds are similar in structure and metabolism to known endocannabinoids, but they do not typically bind as strongly to the main cannabinoid receptors.

Interest in NAAs as endogenous signalling mediators grew after the discovery of AEA (Devane et al., 1992), which led to the discovery and identification of new possible endogenous compounds (Waluk et al., 2014). However, the knowledge on many NAAs is still lacking. Their biological functions and receptors are often unknown and the chemistry behind their biosynthesis and degradation is not fully resolved. All NAAs share the same common substructure R1-CO-NH-R2, and they can be divided into different subcategories by their R1 and R2 structures (Fig. 1).

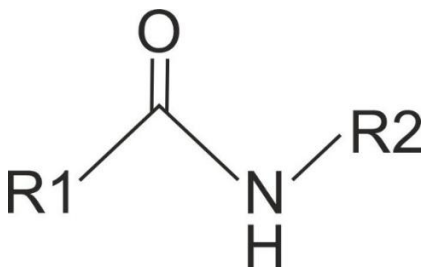

Figure 1. The basic structure of N-acyl amides. R1 represents an acyl tail and R2 amine group.

1.1.1 Primary fatty acid amides

Primary fatty acid amides (PFAMs) have the simplest structure from all the subclasses of NAAs, consisting of a fatty acid linked to a primary amine via an amide bond (Divito & Cascio, 2013). Structural diversity within this group arises from the acyl tail that can vary in length and unsaturation. PFAMs are most known for their sleep-inducing properties. Oleamide, the most extensively studied long-chain PFAM, has also been shown to regulate several other mammalian biological functions, including memory, anti-inflammation and hunger (Akanmu et al., 2007; Martínez-González et al., 2004; Moon et al., 2018; Waluk et al., 2014). These biological functions are induced via oleamide binding to targets, such as CB1 and serotonin receptors, in the brain and CNS (Akanmu et al., 2007; Leggett et al., 2004; Thomas et al., 1997). Oleamide was first identified from a biological source, human plasma samples, in 1989 among other PFAMs that were palmitamide, palmitoleamide, elaidamide, and linoleamide (Arafat et al., 1989). In 1995 oleamide was isolated from the cerebrospinal fluid (CSF) of sleep-deprived cats, and it was shown to induce physiological sleep when injected to rats (Cravatt et al., 1995). This discovery fuelled the interest in PFAMs in biological systems and more compounds were subsequently identified from mammalian CSF and serum (Waluk et al., 2014).

1.1.2 N-acyl amino acids

N-acyl amino acids (NAAAs) are important subclass of NAAs that contribute to many physiological processes especially in the CNS (Waluk et al., 2014). Their basic structure consists of a fatty acid and an amino acid that are linked together via an amino bond. Naturally occurring NAAAs were first identified in mammalian brains in 2001 (Huang et al., 2001). The most notable NAAA identified from this study was N-arachidonoylglycine (NAGly) that was further characterized in detail. As an oxidative metabolite of AEA, NAGly differs structurally by the incorporation of an oxygen atom through oxidation of the ethanolamine moiety (McHugh, Wager-Miller, et al., 2012). *in vivo* and *in vitro* studies have shown that NAGly can also be enzymatically constructed from arachidonic acid and glycine (Bradshaw et al., 2009). Additionally, AEA and NAGly share the same degradation enzyme: fatty acid amide hydrolase (FAAH) to which NAGly was shown to exhibit higher inhibition potency than AEA (Huang et al., 2001). It has been hypothesized that the analgesic and anti-inflammatory effects of NAGly could be partly due to its ability to inhibit FAAH, therefore increasing the levels of endocannabinoids (Grazia Cascio et al., 2004). However, Grazia Cascio et al. (2004) discovered that the FAAH inhibition by NAGly is species-dependent and varies between different tissue

and cell types. It was shown in this study that NAGly is a competent inhibitor of FAAH in rats but not in humans, while N-arachidonoyl-isoleucine (NAIle) was more competent inhibitor of FAAH in humans when compared to rats. This finding suggests that NAIle could increase AEA levels in humans in the same manner as NAGly does in rats, by inhibiting AEA degradation.

Despite the structural similarity between AEA and NAGly, it seems that NAGly does not interact with same receptors or transporters as AEA, suggesting that it functions through different molecular and cellular pathways (Huang et al., 2001). NAGly is generally distributed throughout the mammalian tissues which implies that it could have a role in several biological functions. It has been suggested that NAGly operates through GPR18, GPR55 and GPR92 receptors (Console-Bram et al., 2017; McHugh et al., 2010; Oh et al., 2008). Still, it is important to notice that NAGly can induce other effectors in a GPCR independent manner (Bondarenko et al., 2013; Lu et al., 2013). Its physiological functions are not yet fully characterized but it is known to have analgesic properties and a part in regulation of pain perception (Huang et al., 2001). To this date multiple other NAAAs have been identified and they have been shown to participate in regulation of pain (Huang et al., 2001), anti-inflammation (Burstein et al., 2007), selective inhibition of cancer cell proliferation (Burstein & Salmonsen, 2008), vasodilation (Parmar & Ho, 2010), cell migration (McHugh, Page, et al., 2012; McHugh, Wager-Miller, et al., 2012) and calcium ion mobilization (Kohno et al., 2006).

1.1.3 N-acyl dopamines

N-acyl dopamines (NADs) belong to the subgroup of N-acyl neurotransmitters, which also encompasses other fatty acid–conjugated neurotransmitters, such as histamine and serotonin (Cristino et al., 2020; Mannochio-Russo et al., 2025). They are known for expressing anti-inflammatory and immunomodulatory effects (Navarrete et al., 2010; Sancho et al., 2004). The structure of NADs consists of a fatty acid linked to dopamine via its amino group. These compounds function as agonists to cannabinoid receptors CB1 and CB2 as well as for the transient receptor potential vanilloid type 1 (TRPV1) (Bisogno et al., 2000; Chu et al., 2003). The main identified endogenous TRPV1 ligands are N-arachidonoyl dopamine (NADA) and N-oleoyl dopamine (OLDA) (Chu et al., 2003). TRPV1 has an important role in initiating pain signals and it is predominantly expressed in unmyelinated C-fibre neurons with limited expression in thinly myelinated nerve fibres (Caterina et al., 2000; Kaufman et al., 1982; Kobayashi et al., 2005). The activation of TRPV1 by NADs has been shown to influence pain signalling in inflammatory pain (De Petrocellis et al., 2004; Spicarova & Palecek, 2009).

However, NADs can also produce anti-inflammatory effects in a receptor-independent manner (Navarrete et al., 2010; Sancho et al., 2004). For example, NADA has been reported to inhibit the activation of transcription factors NFκB, NFAT, and AP-1, which are known for inducing inflammation (Sancho et al., 2004). While NADA acts as an agonist for both TRPV1 and CB1 receptors, regulating body temperature and pain perception, OLDA is a strong TRPV1 agonist, whereas its affinity for CB1 is only modest (Bisogno et al., 2000; Chu et al., 2003). Nevertheless, OLDA still mediates similar biological functions to NADA (Chu et al., 2003). Both compounds have been shown to inhibit early and late events in human T-cell activation (Sancho et al., 2004). These findings together suggest that N-acyl dopamines can offer potential neuroprotective effects by modulating different cellular pathways in inflammation.

1.1.4 N-acylethanolamines

N-acylethanolamines (NAEs) are a class of NAAs that consists of ethanolamine linked to a fatty acid via an amide bond (Waluk et al., 2014). Their acyl groups can be unsaturated, saturated or polysaturated which defines their signalling function (Mock et al., 2023). AEA, the first identified endogenous cannabinoid by Devane et al. (1992), remains by far as the most studied endocannabinoid (Scherma et al., 2019). However, despite AEAs popularity among research, rat studies have shown that it only represents under 10 % of all the NAEs in the brain (Cadas et al., 1997; Fontana et al., 1995). The most abundant NAE measured in the mammalian brain is N-palmitoylethanolamine (PEA). Over time, more NAEs have been identified including N-stearoylethanolamine (SEA), N-oleoylethanolamine (OEA), N-linoleoylethanolamine (LEA) and N-docosahexaenoylethanolamine (DHEA) (Mock et al., 2023). NAEs have diverse biological functions that have been shown to regulate inflammation (Dalle Carbonare et al., 2008), appetite (Williams & Kirkham, 1999), anxiety (Kathuria et al., 2003), neurotransmission (Ameri et al., 1999; Musella et al., 2017), fertility (Liu et al., 2002; Rossato et al., 2005), and stress (Hill et al., 2009). Generally, NAEs have been considered to be anti-inflammatory modulators that exhibit their functions through different GPCRs, ion channels, and nuclear receptors (Mock et al., 2023).

As the most studied NAE, AEA is known for regulating multiple biological processes, including pain perception (Calignano et al., 1998; Walker et al., 1999), anxiety (Kathuria et al., 2003), and appetite (Williams & Kirkham, 1999). Its effects are mediated mostly through receptors found in the CNS and the brain (Waluk et al., 2014). “Anandamide”, the common name dedicated to AEA, is derived from the Sanskrit word “ananda”, meaning bliss (Mock et al.,

2023), illustrating its role in promoting anxiolytic, analgesic and antidepressant effects through CB1 signalling in the brain (Gobbi et al., 2005; Hohmann et al., 2005; Kathuria et al., 2003). AEA has been shown to exhibit significantly stronger affinity for the CB1 receptor when compared with the other main cannabinoid receptor, CB2 receptor (Lin et al., 1998). Additional receptors AEA can bind to are TRPV1, transient receptor potential of melastatin type 8 (TPRM8), peroxisome proliferator-activated receptor alpha (PPAR-α) and gamma (PPAR-γ) (Bouaboula et al., 2005; De Petrocellis et al., 2007; Sun et al., 2007; Zygmunt et al., 1999).

PEA was first discovered in 1957 from soybean lecithin, and its anti-inflammatory properties were noted from the very beginning (Kuehl et al., 1957). Later, PEA has been shown to facilitate neuroprotective, analgesic, anorectic and anti-epileptic effects (Lambert et al., 2001; Rodríguez de Fonseca et al., 2001; Skaper et al., 1996). Neuroprotective properties were observed in different disease models, such as Parkinson's and Alzheimer's disease, when PEA was given exogenously (Esposito et al., 2012; Scuderi et al., 2018). PEA is also known to accumulate to the brain or spinal cord following injury and to exert its neuroprotective functions through activating PPAR-α (Franklin et al., 2003; Li et al., 2021; Lo Verme et al., 2005). Both PEA and OEA have been shown to bind to GRP119 (Overton et al., 2006). However, OEA displays clearly a higher affinity to this receptor, which functions as a fat sensor in the gut (Hansen et al., 2012). OEA is most known for regulating feeding behaviour through activation of PPAR-α (Fu et al., 2003), to which it has the strongest affinity out of all the other NAEs (Artmann et al., 2008). Research has shown that during starvation intestinal OEA levels decrease significantly, while AEA levels increase in contrast, indicating a complementary regulation system (Gómez et al., 2002; Rodríguez de Fonseca et al., 2001). Fonseca et al. (2001) found that refeeding the starved mice significantly increased the OEA levels in the small intestine. These findings support the idea, that OEA is a satiety factor, that gets released during food intake. Moreover, it has been found that short- and long-term high fat diets decrease OEA levels in rat jejunum, suggesting that this phenomenon could be the reason for lower satiety and hyperphagia observed in obesity (Artmann et al., 2008; Igarashi et al., 2015).

As many of the NAEs exhibit anti-inflammatory properties, it has been proposed that several of them could potentially have neuroprotective roles (Kleberg et al., 2014). NAE signalling in brain has been shown to play a part in functions such as inflammation, memory formation and stress (Campolongo et al., 2009; Dlugos et al., 2012; Sayd et al., 2015). Consequently, dysregulated NAE levels are implemented in neurological disorders, however, whether they distribute to the severity of the disease or have a protective role remains unclear (Centonze et

al., 2007; Marchioni et al., 2018; Pisani et al., 2010). For example, it has been suggested that AEA itself does not induce disease progression, instead it could act as a neuroprotective agent through CB1 and CB2 activation (Chiurchiù et al., 2018; Gowran et al., 2011). When investigating these compounds, it is important to consider that NAEs can be distributed differently across various tissue types (Mock et al., 2023). This is demonstrated by LEA, which is the most abundant NAE in the gut but significantly diminished in the brain. Thus, it is important to consider the whole NAE profile rather than focusing solely on the limited subset of NAEs when analysing lipidomic measurements.

1.2 Endocannabinoid system

In the 1960s, Δ9-tetrahydrocannabinol was discovered as the main psychoactive component in Cannabis Sativa (Gaoni & Mechoulam, 1964), a plant that has been used as a traditional medicine over a thousand years (Osafo et al., 2021). The corresponding receptors, CB1 and CB2, were identified in the 1990s leading to the discovery of endogenous ligands, AEA and 2-AG, that were given the name "endocannabinoids" (Cristino et al., 2020; Matsuda et al., 1990; Munro et al., 1993). Soon after their identification, it became clear that endocannabinoids and their receptors are important signalling molecules, part of a larger system that came to be known as the ECS. Today, the ECS is known for its vital role in regulating processes necessary for normal physiological function of the body, especially for its role in the immune system (Osafo et al., 2021). Consequently, it also has a major role in various pathological conditions. The ECS is traditionally described as endogenous lipid signalling system comprising two receptors, CB1 and CB2, their endogenous ligands, AEA and 2-AG, and the enzymes involved in their biosynthesis and degradation (Lian et al., 2022). However, recent findings suggest that this classification is too limited, as new bioactive molecules and receptors are discovered interacting with the ECS. As a result, the term ECS was expanded to also encompass the congeners of AEA and 2-AG, NAAs and their metabolites, as well as their associated bioactive enzymes and receptors (Simard et al., 2022). This makes the ECS an even more complex network of numerous overlapping pathways and metabolic processes, thereby complicating its research and understanding.

1.2.1 Endocannabinoid receptors

The ECS, as previously discussed, consists of numerous lipid mediators including various subgroups of NAAs. These compounds exert their properties through different receptors, which

have been shown to exhibit substrate promiscuity among ECS mediators (Cristino et al., 2020). The classical endocannabinoid receptors, CB1 and CB2, are often associated with similar biological functions (Iannotti et al., 2016), although their protein sequences share only 44 % homology (Munro et al., 1993). As members of the large family of GPCRs, both receptors consist of seven transmembrane domains that are linked together by three intracellular and three extracellular loops, featuring an intracellular C-terminal tail and an extracellular N-terminal tail (Iannotti et al., 2016). These two GPCRs primarily couple with inhibitory G-proteins (Lu & Mackie, 2021), and they modify gene expression in the cell by inhibiting adenylyl cyclase and protein kinase A, while inducing mitogen-activated protein kinase (De Pol & Kolla, 2021). Additionally, they can inhibit specific voltage-sensitive calcium channels, stimulate inwardly rectifying potassium channels and recruit beta-arrestins (Lu & Mackie, 2021), which are proteins known for regulating GPCR signalling (Kee et al., 2024).

CB1 is the most abundant GPCR in the mammalian brain and it is widespread across the CNS and peripheral nervous system (Herkenham et al., 1990; Turu & Hunyady, 2010). Its role in maintaining homeostasis is highlighted by its expression in nearly all mammalian tissues and organs. It has been shown that CB1 receptors are predominantly located presynaptically in both excitatory and inhibitory neurons within CNS (Katona & Freund, 2008; Mátyás et al., 2008). However, they can also be expressed postsynaptically in the CNS (Rodríguez et al., 2001), as well as in non-neuronal cells in the brain, where they promote neurotransmitter release (Navarrete & Araque, 2008; Stella, 2010). CB1 receptors have also been shown to be expressed on the enteric nerves in the submucosal and myenteric plexuses in the small intestine, with especially high abundance in the nerve fibres in lamina propria (Cuddihey et al., 2022). The localization of CB1 receptors in the enteric nervous system (ENS) could be an indication for their important role in the regulation of gastrointestinal (GI) functions. In addition to existing as a homodimer, CB1 can heterodimerize with other GPCRs, such as D2 dopamine and opioid receptors, enhancing its already wide signalling potential (Przybyla & Watts, 2010; Rozenfeld et al., 2012). Both, CB1 and CB2 signalling, can be further regulated by positive and negative allosteric modulators, adding to the complexity of ECS (Nguyen et al., 2017).

Unlike CB1, CB2 is expressed at low levels in the brain, predominantly in the microglia, with some expression detected also in astrocytes and neurons (Grabon et al., 2024). However, CB2 is expressed in most immune cells (Graham et al., 2010). Its activation has been shown to reduce the release of pro-inflammatory cytokines and lymphangiogenic factors in human lung macrophages (Staiano et al., 2016). CB2 receptors are expressed in peripheral organs, that have

a part in immune response, for example in the spleen, thymus and tonsils (Galiègue et al., 1995). It was reported that the amount of CB2 mRNA in spleen and tonsils was equivalent to the amount of CB1 mRNA in the CNS. Overtime CB2 has been recognized as an important immune modulator which responses depend on the immune cells and properties of inflammatory responses (Bala et al., 2024). When activated these receptors inhibit the production of inflammatory mediators and they can mediate immune cell migration by altering chemotaxis, which affects the severity and the duration of inflammation. Alongside the main and most studied endocannabinoid receptors, other putative receptors have been discovered, which exhibit endocannabinoid-like receptor activity (Lian et al., 2022). TRPV1, PPARs, GPR18, GPR55 and GPR119, are all receptors considered to be a part of the ECS.

TRPV1 belongs to a group of ion channel receptors, and it is expressed widely across several central and peripheral organs (Alawi & Keeble, 2010). Although, it is a non-selective cation channel, it shows a preference for calcium (Owsianik et al., 2006). TRPV1 can be activated by several factors, including exogenous compounds like capsaicin and endogenous ligands called endovanilloids, which for instance include AEA and other NAEs (Darré & Domene, 2015; De Petrocellis et al., 2001; Movahed et al., 2005). Additionally, other chemical and physical stimuli, such as low pH and high temperatures, have been shown to activate TRPV1 channels (Tominaga et al., 1998). TRPV1 activation is commonly associated with pain transmission and neurogenic inflammation (Julius, 2013). It is also shown to play a role in neuronal overexcitability, synaptic plasticity and neurotoxicity (Bennion et al., 2011; Iannotti et al., 2014; Shen et al., 2025). TRPV1 is expressed throughout the CNS (Martins et al., 2014), but it is also found abundantly in C-type sensory nerve fibres in dorsal root ganglia (Kobayashi et al., 2005). Its expression is not limited to neural sites as it extends to non-neural cells and tissues (Kudsi et al., 2022). In sensory neurons TRPV1 channels have a role in combining various sensory inputs to modify and transmit pain signalling (Caterina et al., 2000). In central neurons, these channels are located pre- and post-synaptically, contributing to the regulation of synaptic signalling strength (Bennion et al., 2011). Notably, this regulation influences processes such as pain, anxiety and depression, typically producing effects opposite to those of CB1 receptors (Iannotti et al., 2016).

The nuclear hormone receptor family of PPARs comprises three isoforms, PPAR-α, PPAR-β/δ and PPAR-γ, which function by forming heterodimers with the retinoid X receptor (O'Sullivan, 2016). These heterodimers influence gene expression by binding to PPAR response elements in the DNA. Genes regulated by PPARs are known to act in the regulation of inflammation,

metabolism, energy homeostasis and cell differentiation. PPARs can be activated by various endo- and exogenous ligands that differ in their chemical structure. The endogenous ligands of PPARs include fatty-acids, endocannabinoids and endocannabinoid-like mediators (Lian et al., 2022). PPAR-α is activated by several NAEs, among endocannabinoid-like mediators OEA and LEA have been shown to be the most effective (Artmann et al., 2008). The α-isoform is highly expressed in the GI tract, liver and brown adipose tissue, where it controls lipid metabolism (Lian et al., 2022). As a strong PPAR-α agonist, OEA has been shown to decrease obesity and induce satiety through activation of this receptor isoform (Fu et al., 2003). Additionally, PPAR-α and PPAR-γ are expressed in the brain where they induce neuroprotective and anti-inflammatory effects during acute and chronic neuroinflammation (Cristino et al., 2020). PPAR-γ isoforms are highly expressed in the adipose tissue, where they regulate differentiation of adipocytes and maintain glucose and lipid homeostasis (Lian et al., 2022). AEA has been shown to be potent PPAR-γ ligand, while some evidence also suggests that NADA, PEA and OEA could activate PPAR-γ (O'Sullivan, 2016). There is also evidence that some endocannabinoid degradation metabolites are PPAR activators. For example, even though AEA does not bind to PPAR-β/δ, its derivative metabolite arachidonic acid does (Yu et al., 2014).

GPR18, GPR55, and GPR119 have emerged as candidate receptors within the ECS (Lian et al., 2022). GPR55 is mainly expressed in the CNS, pancreas and liver, and is linked to biological processes, such as energy metabolism and inflammation (Jin et al., 2024). Although L-α-lysophosphatidylinositol is considered GRP55s endogenous ligand, the receptor can be activated by endocannabinoids (Lian et al., 2022). GRP119 is expressed in various organs, where it has been shown to influence multiple biological processes, including inflammation, appetite, along with glucose and lipid metabolism (Jin et al., 2024). Among ECS mediators, OEA has been identified as an endogenous ligand of GRP119, regulating secretion of incretin in the GI tract and insulin in pancreas (Lian et al., 2022). GRP18 has only recently been regarded as a putative cannabinoid receptor for its interactions with other synthetic, endo- and exogenous cannabinoids. From NAAs, NAGly, has been demonstrated as a natural ligand of GRP18 (Kohno et al., 2006). This receptor has been found to be abundant in various human tissues, including the hypothalamus, GI tract and white adipose tissue. Additionally, GRP18 is highly expressed in immune cells, where it influences their proliferation, migration and infiltration and has a role in mediating anti-inflammatory responses (Lian et al., 2022).

1.2.2 Endocannabinoid metabolism

With numerous key players ECS consists of diverse metabolism networks, including different biosynthesis and degradation pathways. Some of these routes have been described in great detail while others are yet to be discovered. The biosynthesis of AEA and other NAEs fall under the more well studied pathways in the ECS. NAE biosynthesis can proceed through four different routes, which all have the same common precursor, N-arachidonoyl-phosphatidylethanolamine (NAPE) (Simard et al., 2022). The most straightforward pathway is catalysed by NAPE-specific phospholipase D (NAPE-PLD), which hydrolyses the NAPE releasing a NAE in one step reaction (Tsuboi et al., 2018). The other three alternative pathways have multiple catalysation reactions independent of NAPE-PLD (Simard et al., 2022). The importance of NAPE-PLD dependant pathway in NAE biosynthesis was shown in Leishman et al. (2016) study, in which NAPE-PLD knockout mice had significantly reduced NAE levels when compared to the wild type. Additionally, they also measured the changes of other NAA levels, which were affected by the deletion of NAPE-PLD. These findings together demonstrate that NAPE-PLD influences the wider ECS and its impact is not limited to the NAEs only.

NAEs are degraded into free fatty acids and ethanolamine through hydrolysis (Tsuboi et al., 2018). This reaction can be catalysed by FAAH, FAAH-2 or N-acylethanolamine acid amidase (Simard et al., 2022). In 1996, FAAH was molecularly characterised and proposed as a general degradative enzyme for fatty acid amide family of signalling molecules (Cravatt et al., 1996). This idea was supported by *in vivo* experiments, using both mice treated with FAAH inhibitors and FAAH knockout mice, which showed impaired fatty acid amide degradation activity and accumulation of NAEs (Cravatt et al., 2001). FAAH-2, sharing 20 % sequence identity with FAAH, was discovered in 2006 (Wei et al., 2006). Despite low sequence identity, both of these enzymes belong to the amidase signature enzyme family and contain the serine-serine-lysine catalytic triad as well as other catalytically important residues, which are essential for amide bond hydrolysis. Interestingly, FAAH-2 is found in primates but not in murids, unlike FAAH, which is well-conserved in mammalians. FAAH-2 favours monounsaturated NAAs, such as oleamide and OEA, while having low selectivity for AEA, which has polyunsaturated acyl tail. N-acylethanolamine acid amidase is a lysosomal enzyme that doesn’t share sequence identity with FAAH (Tsuboi et al., 2018). However, it can hydrolyse AEA and other NAEs at acidic pH, especially PEA which it shows significantly higher activity (Ueda et al., 2001).

1.2.3 Endocannabinoid system and the gastrointestinal tract

Interest in the physiological role of ECS in the GI tract has increased in the recent years, driven by the discoveries revealing that its components do localize and exert their functions in this system (Lian et al., 2022). CB1 has been well established in the ENS where it regulates processes such as GI motility and intestinal permeability (Sharkey & Wiley, 2016). Cuddihey et al. (2022) demonstrated that CB1 can restore gut barrier integrity after it has been disturbed by high fat diet. The CB2 receptor has been also identified in the ENS as well as in immune and epithelial cells in GI tract (Sharkey & Wiley, 2016). This receptor has been shown to exhibit anti-inflammatory properties that restore gut function after inflammatory stress (Mathison et al., 2004). Furthermore, both cannabinoid receptors and endocannabinoids have been shown to impact human GI tract function in a manner that indicates their possible immunomodulatory and protective roles (Wright et al., 2005). In addition to the main cannabinoid receptors, the GI tract also expresses other receptors belonging to the ECS (Lian et al., 2022). These receptors have been shown to influence a variety of functions in GI tract, including energy homeostasis and inflammation.

Recent studies have provided evidence that the ECS signalling in the GI tract is not limited to local regulation but also affects the CNS through the gut-brain axis (Berland et al., 2022; Chevalier et al., 2020; Dohnalová et al., 2022). The gut-brain axis is considered to consist of humoral and neural networks that connect the two systems (Storr & Sharkey, 2007). ECS signalling between the gut and brain is largely mediated through the vagus nerve. Berland et al. (2022) demonstrated that vagus-mediated CB1 signalling is essential for binge eating behaviours in mice. They observed that peripherally restricted CB1 antagonists reduced binge eating consumption in mice and that vagal integrity was essential for this effect to take place, since the same reduction was not observed in mice with impaired vagal nerve. While providing evidence for the crucial role in disordered eating, this finding suggests that the ECS gut-brain transmission may also influence feeding behaviour more broadly.

Gut microbiome has been shown to influence the gut-brain communication as well, adding further complexity to the investigated system (Chevalier et al., 2020; Dohnalová et al., 2022). The human gut microbiome has been estimated to consist of approximately 100 trillion bacterial cells that form a mutually beneficial ecosystem with the host (Cani et al., 2016). This mutual relationship provides the host with additional metabolic and genetic capacity. Consequently, around 10% of the hosts intestinal transcriptome is considered to be regulated by the microbiota.

The gut microbiota can modulate the mood and behaviour, as demonstrated in studies focusing on depressive-like behaviours and exercise motivation in mice (Chevalier et al., 2020; Dohnalová et al., 2022). Chevalier et al. (2020) found that faecal microbiota transplantation from mouse models of depression to germ-free mice induced depressive-like behaviours in the recipients. Additionally, they observed that the change in behaviours was reversible by both administration of endocannabinoid precursor, arachidonic acid, and *Lactobacillus plantarum* strain. Dohnalová et al. (2022) reported microbiome-dependent gut-brain pathway that employs NAAs to regulate the motivation for exercise. In their study they found that depletion of gut microbiota with antibiotics led to significant loss of running distance in mice, which was also observed as impaired striatal dopamine response. The most potent metabolites from the microbiome to activate dorsal root ganglion neurons were identified as NAAs. Intestinal caecal samples showed that OEA levels were significantly reduced in mice treated with antibiotics and that the OEA abundance correlated positively with the running distance. Furthermore, they demonstrated that mice lacking large fraction of spinal and vagal afferent neurons that express TRPV1 were similarly impaired in exercise as the mice treated with antibiotics. Notably, this effect was not further emphasized by antibiotic treatment. These findings together suggests that microbiome produces intestinal NAAs, that activate sensory neurons which relay the signal to the brain, leading to enhanced physical endurance via increased dopamine signalling. Overall, the research presented here indicates the existence of a complex intertwining system, where vagus mediated gut-brain signalling is affected by metabolites produced by the gut microbiota such as NAAs. The mechanisms that drive these interactions need to be further investigated to better understand the role of each component and the effects on microbial and host metabolism and physiology.

1.3 Mass spectrometric analysis of N-acyl amides from biological matrices

As the interest in compounds belonging to the ECS has grown over the years, the development of methods targeting their analysis from biological matrices has advanced as well (Marchioni et al., 2018). Liquid chromatography-tandem mass spectrometry (LC-MS/MS) has become the standard approach for its high sensitivity and selectivity, as well as for its compatibility with the physicochemical properties of endocannabinoids and related compounds. Techniques based on liquid chromatography coupled with mass spectrometry (LC-MS) aim to separate and identify the analytes from the samples (Gross, 2017). The separation is a consequent of different compounds in liquid mobile phase interacting with the stationary phase material of the chromatographic column in different affinities causing them to elute in different times. The

time that it takes for a compound to travel through the column is referred to as its retention time, which remains reproducible while the chromatographic conditions stay unchanged. After the chromatographic separation, the analytes are directed into a mass spectrometer for the detection. In mass spectrometry (MS), the aim is to generate ions from the analytes and to separate and detect them based on their *mass-to-charge ratio* (*m/z*). Tandem mass spectrometry (MS/MS) acquires two consecutive levels of *m/z* analysis, MS1 and MS2. The first level, MS1, produces precursor ions and selects them by their *m/z* values to be further analysed. Selected precursor ions are then fragmented once again, producing product ions that can be detected in MS2. Each level in MS/MS adds to the selectivity of the analysis by monitoring specific ions, thus reducing interference from matrix components. Therefore, MS/MS is ideal for analysis of compounds that exist only in trace amounts in samples. Indeed, sub-trace levels of endogenous compounds, such as endocannabinoids, in biological samples and their low chemical stability are known to make their detection challenging (Marchioni et al., 2018). Additionally, biological samples may contain other endogenous compounds that can co-elute with the target analytes disturbing and impairing the quality of the analysis. In metabolomics studies the quality of the samples, especially sample collection and preparation methods, significantly influence the data obtained from the analysis (Eshawu et al., 2025). Therefore, thoroughly optimized sample preparation method is crucial for reproducible and robust data.

1.3.1 Sample preparation

The aim of metabolomics sample preparation is to preserve the target analytes as they were at the moment of sample collection to maintain biological accuracy throughout the analysis (Eshawu et al., 2025). As metabolites are known to be afflicted by pH, temperature, enzymes and sample processing time, ensuring proper collection and preparation methods is critical when handling biological samples. To avoid degradation and transformation of target metabolites, fast collection combined with on-spot freezing and –80 °C storing is the standard practice.

Besides metabolites, biological samples are abundant in various other biomolecules, salts and inorganic compounds, which makes them highly complex matrices (Niu et al., 2018). These interfering molecules can cause ion suppression or enhancement in MS analysis, which distorts the detected signal compromising analytical reliability (Eshawu et al., 2025). Therefore, biological samples require preparation methods that eliminate the disruptive compounds while preserving the target analytes. Protein precipitation with organic solvent and filtration are the

most common methods used in LC-MS analysis to remove proteins, particulates and microbial contaminants from the samples. Protein precipitation is especially favourable method when the target compounds are vulnerable to heath and changes in pH (Niu et al., 2018). The organic solvent causes the protein denaturation and aggregation, separating them from the analytes dissolved into the liquid phase. Despite being non-selective method, protein precipitation has become routine practise since it is simple and fast to conduct, plus it requires minimal equipment.

1.3.2 Liquid chromatography-tandem mass spectrometry

LC-MS techniques have been well established in the field of metabolomics due to the conveniency they bring to the analysis process (Eshawu et al., 2025). The capability to analyse thermolabile, polar and non-polar analytes without derivatization provides a platform to investigate a wide range of compounds. Furthermore, LC-MS/MS specifically has become the standard technique for detecting endocannabinoids from biological samples (Marchioni et al., 2018). This can be attributed to its high throughput capability combined with its enhanced selectivity and sensitivity. Reverse phase columns with C18 stationary phase are commonly employed when separating endocannabinoid-like compounds due to their lipophilic characteristics (Zoerner et al., 2011). The elution system for these nonpolar compounds can be either gradient or isocratic, with mobile phase consisting of organic and aqueous solvents with additives (Marchioni et al., 2018). Formic acid is often used as an additive at low concentrations (Zoerner et al., 2011), as it promotes positive ion formation of basic compounds during MS analysis (Marchioni et al., 2018). Standard isocratic elution for endocannabinoid separation uses a methanol-water mobile phase, with methanol accounting for 85–90 % (Zoerner et al., 2011). The percentage of organic solvent, such as acetonitrile or methanol, is increased during gradient elution. Its proportion in the mobile phase is increased typically from 10–65 % up to 90–100 %. A recent systematic review of targeted LC-MS/MS methods found that electrospray ionization (ESI) in positive mode is the most commonly used ionization method for endocannabinoids and NAEs (Amir Hamzah et al., 2025). ESI is considered a soft ionization technique that generates gas phase ions with minimal fragmentation from the analytes dissolved in the liquid mobile phase (Gross, 2017). Overall, the systematic review concluded that the LC-MS/MS methods for the analysis of these compounds were relatively consistent between different biological matrices (Amir Hamzah et al., 2025). Moreover, they emphasized that the differences in methods mainly stemmed from sample preparation protocols.

1.3.3 Faecal sample analysis

Analysing biofluids offers valuable information about the physiological environment that surrounds them as well as the tissue that they are produced in (Karu et al., 2018). To investigate complexity of intertwined GI tract–microbiome biosystem, faecal matter has risen as an advantageous biospecimen in metabolic analysis. While LC-MS represents the most extensively utilized method in metabolomics analysis, it has not been as widely applied in faecal analysis (Deda et al., 2015). Moreover, the methods for sample collection and preparation are lacking in standardization (Karu et al., 2018). The absence of standard protocols is aggravated by the heightened vulnerability of faecal analysis to differences in methodologies. Unlike other biofluids, faeces are a semi-solid biological matrix that consists of both endogenous and exogenous matter which complicates the establishment of routine processes.

Gut microbiome together with GI tract shape the diverse compound profile of faecal matter through processes such as ingestion, digestion, and absorption (Karu et al., 2018). Typically, faeces are composed of 63–85 % water, while bacterial biomass accounts for the most of the dry weight (25–54%). The remainder consists of undigested dietary residues, shed colonic epithelial cells, macromolecules, and lastly metabolites which make up the faecal metabolome. Post-collection faecal samples are sensitive to alterations in metabolite profile due to microbial fermentation, that can be accelerated by external factors, such as temperature changes and aerobic conditions. Therefore, sample preparation protocol must be replicable, short, and able to extract all of the metabolites as they were at the point of collection (Deda et al., 2015). Most commonly the samples are frozen after collection to avoid deterioration. Sample preparation steps for the LC-MS analysis typically involve dilution into an organic solvent, such as methanol, followed by centrifugation to remove proteins and precipitants, and filtration to prevent column blockage. The high sensitivity of LC-MS instruments offers wide metabolite coverage, detecting thousands of signals in faecal samples. However, this leads to an immense amount of data that requires careful processing and interpretation to identify the true metabolites from the co-eluting compounds, without confusing different isotopes, adducts and fragment ions as separate metabolites (Karu et al., 2018). Developing targeted LC-MS/MS methodologies represent a promising approach for identification of specific metabolites in faeces. Targeted multiple reaction monitoring (MRM) analysis provides higher sensitivity and broader detection range than the untargeted analysis. MRM analysis tracks the transitions of multiple predefined precursor ions and their corresponding product ions within a single analysis cycle to acquire more reliable data from the chosen analytes, while in turn sacrificing the

detection of non-target ions (Gross, 2017). To develop a reliable and robust MRM method requires availability of well-characterized reference standards and time-consuming optimization of the chromatographic separation, MRM channels and MS conditions (Karu et al., 2018). Even with a well-optimized method, the interpretation of the analysis results can still be rather complicated (Deda et al., 2015). Metabolites in faecal samples can originate from the host or microbial metabolism, or they can be produced via co-metabolism. Furthermore, these metabolites are engaged in a constant dynamic interplay between the GI tract and the gut microbiota. As a consequence, faeces represent a biospecimen with vast and unique metabolic information, deserving of further investigation.

1.4 Microbiome-derived N-acyl amides

Gentry et al. (2024) demonstrated the advantage of reverse metabolomics for the annotation of NAAs in large untargeted metabolomics datasets. The reverse metabolomics approach they introduced searches public untargeted MS/MS data to see if specific fragment spectra can be found and identified. To obtain the MS/MS fragment spectra for NAAs they used combinatorial synthesis to link together 46 fatty acyl chlorides with 32 amines. Over 60,000 spectral matches were made with the created NAA library when searching through 25,463 datafiles. Most of the matches came from animal databases, especially from human and mice. The NAAs were predominantly detected in faecal, caecum and skin samples. Additionally, they detected variety of NAAs from microbial datasets. Another recent metabolomics focused study discovered 777 previously undocumented NAAs from public LC-MS/MS untargeted datasets (Mannochio-Russo et al., 2025). 18% of these compounds were derived from short-chain fatty acids and were present in the GI tract as well as other organs in humans and rodents. In their study, Mannochio-Russo et al. (2025) hypothesised that these NAAs could be partially produced by the microbiota. Evidence for this claim was gathered from public datasets as well as human gut bacteria cultures, which showed that these microbes can produce NAAs, if both amine head and lipid tail groups are available as substrates. Antibiotic use, diet, and health conditions were also shown to affect the NAA levels. These findings align with an earlier study, where Cohen et al. (2017) observed that human gut microbiota produces NAAs which interact with GPCRs, such as GPR119. Their findings revealed that NAA synthase genes are particularly enriched in human gut microbes and that the NAAs they produce are structurally similar to the endogenous GPCR ligands.

Over the years, NAAs have gained attention due to their established roles as endogenous lipid signalling molecules, participating in essential biological pathways (Bradshaw & Walker, 2005; Waluk et al., 2014). However, the recent research has accumulated strong evidence for gut microbiota-derived NAAs, that can potentially influence the host physiology (Cohen et al., 2017; Dohnalová et al., 2022; Mannochio-Russo et al., 2025). In particular, Gentry et al. (2024) and Mannochio-Russo et al. (2025) revealed the large-scale information within untargeted metabolomics data providing extensive insights into NAAs. Out of over 1,400 synthesized NAAs, a third were detected from the public metabolomics datasets, highlighting both the vast size and structural diversity of the NAA family. Understanding the complexity and function of NAAs is crucial, as many of these compounds are an essential part of the signalling pathways and biological processes. Therefore, further research is required to uncover their potential in human physiology, including gut microbiome, GI tract and ECS.

1.5 Aims of the thesis

To chemically synthesize two NAAs, Arg-C18:0 and histamine-C5:0, and utilize them as qualitive standards in targeted scheduled MRM (sMRM) analysis.

To detect NAAs from human faecal samples using the targeted sMRM analysis.

2 Materials and methods

2.1 Chemical reagents

Synthesis reagents, L-arginine ≥ 98 %, histamine ≥ 97 %, valeric acid ≥ 99 %, stearic acid ≥ 98.5 %, ethyl chloroformate ≥ 98 %, triethylamine ≥ 99%, and sodium hydroxide 99–100 %, were purchased from Sigma-Aldrich (Saint Louis, MO, USA). Tetrahydrofuran ≥ 99.9 % was from VWR Chemicals (United Kingdom).

Synthetic NAA standards were provided by Dorrestein Lab, University of California (Gentry et al., 2024). The standards were mixtures of compounds produced by the conjugation of 46 fatty acid chlorides with 31 amines, resulting in total of 1,426 NAAs.

Internal standards (IS), Arachidonoyl ethanolamide d8 (AEA-d8), Alpha-linolenoyl ethanolamide d4 (aLEA-d4), Oleoyl ethanolamide d4 (OEA-d4) and Stearoyl ethanolamide d3 (SEA-d3), were purchased from Cayman Chemical Company (Michigan, USA) or Sigma-Aldrich (Saint Louis, Missouri, USA).

Ultrapure methanol (MeOH) ≥ 99.9 %, ultrapure acetonitrile (ACN) ≥ 99.9 %, 2-propanol (IPA) ≥ 99.9 %, and ultrapure water, were from Honeywell Riedel-de Haën^{TW} (Charlotte, NC, USA). Formic acid ≥ 99 %, was from VWR Chemicals (United Kingdom).

2.2 Synthesis of histamine-C5:0 and arginine-C18:0

Combinatorial reactions protocol for N-acyl amides by Gentry et al. (2024) was modified and applied to synthesize histamine-C5:0 and Arg-C18:0. Activation solutions for the fatty acids were prepared by mixing 1 ml of tetrahydrofuran with 0.1 mmol of fatty acid, 0.15 mmol of ethyl chloroformate and 0.14 mmol of triethylamine. The mixtures were put on a shaker for 30 min at room temperature. 0.1 mmol of each amine was dissolved in separate vials containing 1 ml of 0.1 M NaOH and combined with the corresponding fatty acid solution. Both mixtures were shaken in room temperature for 1-2 hours. 3:50,000 (v/v) dilutions were prepared in ACN/H_2O (30/70, v/v) and they were filtered through 0.20 µm Minisart RC 15 single use syringe filters (Startorius Stedim biotech GmbH, Gottingen, Germany).

2.3 Faecal samples

Faecal samples (n=40) from cohort consisting of 5.5-year-olds, with equal representation of both sexes were provided by FinnBrain. The samples were homogenized prior to sample

preparation. Pooled quality control (QC) sample was prepared by adding 20 µl of each sample together.

2.4 Sample preparation

Internal standard (IS) solvent consisting of 25 ppb AEA-d8, 25 ppb aLEA-d4, 100 ppb OEA-d4 and 100 ppb SEA-d3 was prepared in MeOH/ACN (5:1, v/v) with 0.1 % FA.

Samples for targeted sMRM LC-MS/MS were prepared by adding 120 µl of homogenized faecal samples and synthetized NAA dilutions each to 600 µl of IS solvent, vortexed and filtered through a protein precipitation filter plate (Merck, Darmstadt, Germany). Blanks consisting of MeOH and blanks consisting of IS solvent were treated the same as the samples. Filtrates were collected into total recovery glass vials. Additional blanks consisting of 600 µl of IS solvent were prepared without the filtration step into the glass vials. Samples were dried under a stream of nitrogen at 40 °C and resuspended into solvent mixture consisting of 70 % MeOH/ACN (5:1, v/v) and 30 % of 0.1 % FA in water. Standard NAA mixtures spiked with IS solvent were evaporated under a stream of nitrogen at 35 °C and resuspended into the same solvent mixture as the samples, resulting in 1:10 dilutions of the original standard mixtures provided by Dorrestein.

2.5 Nuclear magnetic resonance spectroscopy

The non-diluted synthesis mixtures were dried under a stream of nitrogen at 35 °C. The dried Arg-C18:0 sample was dissolved into 700 µl 99.80 % Methanol D4 (Eurisotop, Saint-Aubin, France) and + 200 µl 99.80 % Chloroform D + 0.03 % TMS (Eurisotop, Saint-Aubin, France) v/v. The dried histamine-C5:0 sample was dissolved into 700 µl Methanol D4. Nuclear Magnetic Resonance (NMR) analysis was performed with AV500Cryo (Bruker BioSpin, Ettlingen, Germany), featuring Bruker 500 MHz magnet and liquid nitrogen cooled CryoProbe.

2.6 Liquid chromatography conditions

The ultra-performance liquid chromatography (UPLC) instrument utilized was ACQUITY premier system (Waters, MA, USA). Reverse-phase liquid chromatography was accomplished by using Phenomenex Kinetex 1.7 µm 100 x 2.1 mm XB-C18 100 Å column with Phenomenex SecurityGuard ULTRA Cartridge pre-column that were held at 40 °C. Mobile phase A, 0.1 % FA in water, and mobile phase B, MeOH/ACN (5:1, v/v), were used as the eluents and the flow rate was 0.4 ml/min. Gradient elution conditions for the run are presented in the Table 1.

Injection volume was 10 µl and the autosampler was set at 15 °C, wash solvent consisted of 0.1 % FA in H_2O/ACN/IPA (3:5:2 v/v) and the post-injection wash time was 8 s.

Table 1. Gradient elution conditions for the ultra-performance liquid chromatography.

The table presents mobile-phase gradient of aqueous (%A) and organic (%B) solvent ratios as a function of time.

Time (min)	%A	%B
0	95	5
12.92	15	85
13.92	0	100
17.42	0	100
17.62	95	5
21	95	5

2.7 Untargeted mass spectrometry settings

Mass spectrometric detection was conducted on a ZenoTOF 7600 (Sciex, Framingham, MA, USA) with an electrospray ion (ESI) source and collision-induced dissociation (CID) fragmentation. Scan type was time-of-flight (TOF) on a positive mode, with IDA acquisition. Temperature was set on 300 °C and the pressure of ion source gas 1 and 2 were 50 psi and 70 psi, respectively. Spray voltage was 5500 V, scan range was set at 50–600 *m/z*, collision energy (CE) was 35 V and declustering potential was 80 V. Sciex ESI positive calibration solution X500B was used for the calibration of the mass scale.

2.8 Targeted mass spectrometry settings

sMRM method was utilized in targeted mass spectrometric analysis on ZenoTOF 7600 with an ESI source and CID fragmentation. Retention time windows were set ± 12 s around the expected retention time for each compound (Table A1). The scan range was set from 50 *m/z* to the targeted NAAs precursor *m/z* and the CE was set at 25 or 35 for each compound (Table A1). Other parameters were same as in untargeted analysis.

2.9 Data processing

Data processing was conducted with Sciex OS software (Framingham, MA, USA). Features were annotated using the retention times as well as precursor and fragment ion *m/z* values of

standard NAA mixtures and in-house synthesized NAAs (Table. A1). Precursor ion mass error limit was set at ± 10 ppm for the peak to be considered valid. 3:1 signal to noise ratio was applied in determination of peaks.

2.10 Statistics

Data representing relative abundances of NAAs between sexes was visualized with boxplots generated in R version 4.5.2 (R Core Team, 2025) using ggplot2 package (Wickham H, 2016). The Mann-Whitney U test was used to evaluate differences between sexes, with a p-value below 0.05 considered significant.

2.11 Artificial intelligence

Artificial intelligence was not used in the thesis.

3 Results

3.1 Chemical synthesis of histamine-C5:0 and arginine-C18:0

Combinatorial reaction strategy utilized by Gentry et al. (2024) was modified and implemented to synthetize two in-house NAA standards, histamine-C5:0 and Arg-C18:0, separately (Fig. 2). Histamine-C5:0 belongs to the subgroup of N-acyl neurotransmitters and consists of a histamine conjugated to valeric acid. Histamine-C5:0 represents the smaller side of NAAs while Arg-C18:0 represents the opposite, with arginine bind to the 18-carbon long stearic acid. Besides the differences in acyl tail lengths, the amide head groups differ from each other in their chemical properties. Histamine is a polar molecule, consisting of an aromatic imidazole ring connected to an ethylamine, whereas arginine is a highly basic compound with positively charged guanidinium group.

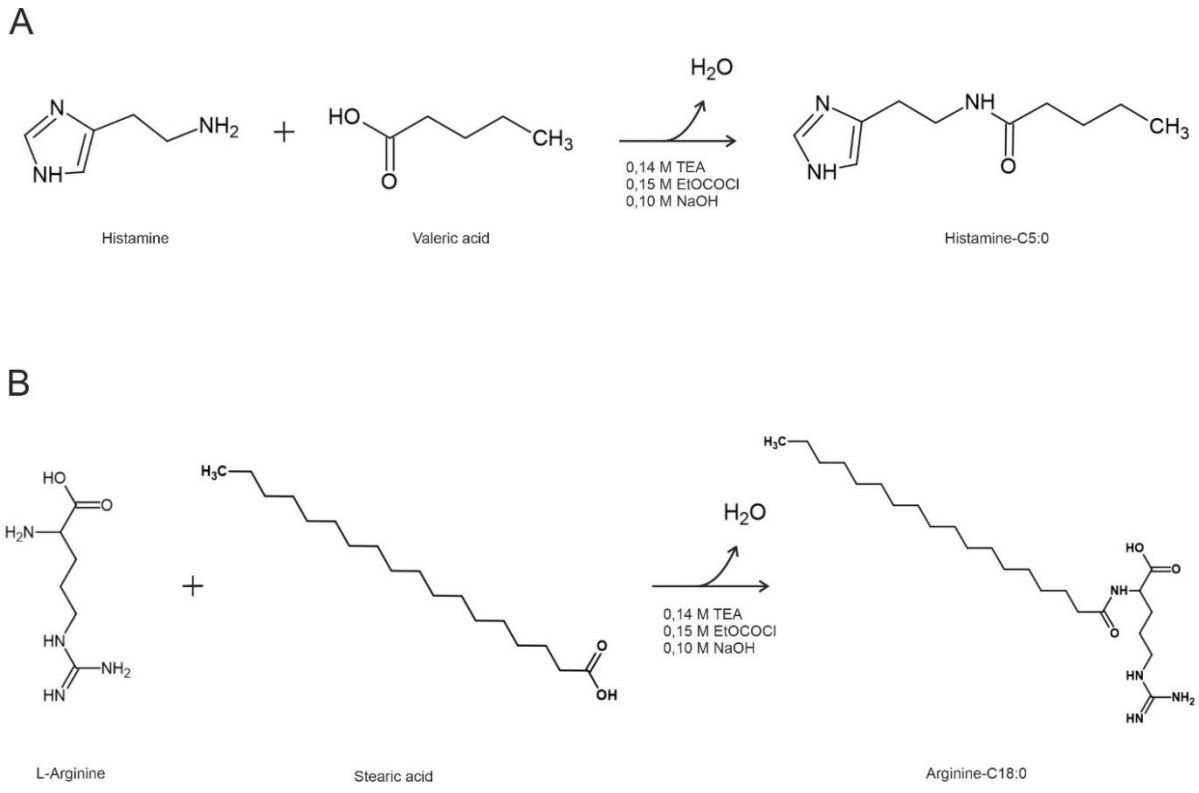

Figure 2. Chemical synthesis reaction schemes of A) histamine-C5:0 and B) Arg-C18:0. TEA stands for triethylamine and EtOCOCl for ethyl chloroformate. Tetrahydrofuran was used as reaction medium.

3.1.1 Mass spectrometry analysis

To verify that the syntheses were successful, the reaction mixes were analysed with LC-MS/MS. The in-house standards were compared with a synthetic NAA standard mixture from Dorrestein Lab (University of California). This particular mixture contained the target NAAs, as well as over 400 other NAAs since their synthesis was performed simultaneously in a single combinatorial reaction mixture. The identification of the newly synthesized NAAs was based on retention time and ion fragment profile matching.

Extracted ion chromatogram (XIC) of the in-house histamine-C5:0 at *m/z* 196.14 obtained with LC-MS analysis showed peak splitting, with more intense peak at 0.554 min and smaller peak at 1.266, the mass errors for them were 0.2 and -0.2 ppm respectively (Fig. 3). However, both peaks were also observed in the standard mixture, with mass errors of 0.3 ppm for the first and 0.7 ppm for the second peak. Additionally, all of the peaks presented nearly identical fragmentation profile, with most intense matching ion fragments at *m/z* 95.0601 and 112.086 (Fig. A1). The in-house histamine-C5:0 had significantly higher intensity in the first peak compared to the one from NAA standard mixture, while the signals from the second peaks were similar between the two. The retention times were also comparable, with minor differences in the peak shapes, resulting in slight variation in the measured times. The exact fragments were further annotated using Sciex OS software, utilizing a mol-file that contained the structure of the histamine-C5:0 (Fig. 4). The software's integrated fragment ion prediction tool generated theoretical fragment ions from the imported mol-file and matched them to the MS/MS spectra based on the *m/z* values. There was no precursor ion detected in the fragment profile. The most intense fragments contained the imidazole ring and part of the carbon chain from the amine head group. The less intense ion at *m/z* 57.0694 corresponds to the acyl tail fragment.

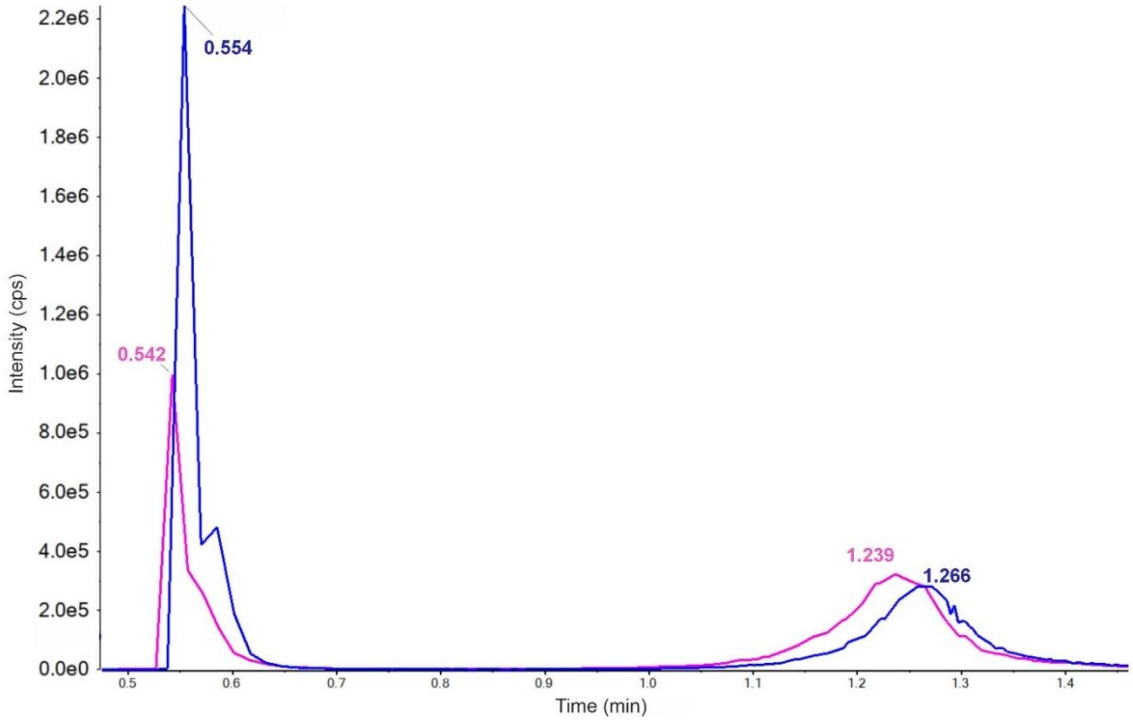

Figure 3. XICs of in-house (blue) and standard mixture (pink) histamine-C5:0 at *m/z* 196.14 obtained with LC-MS analysis. Reverse-phase C18 column (Phenomenex Kinetex 1.7 µm 100 x 2.1 mm XB-C18 100 Å column with Phenomenex SecurityGuard ULTRA Cartige pre-column) was used in UPLC separation.

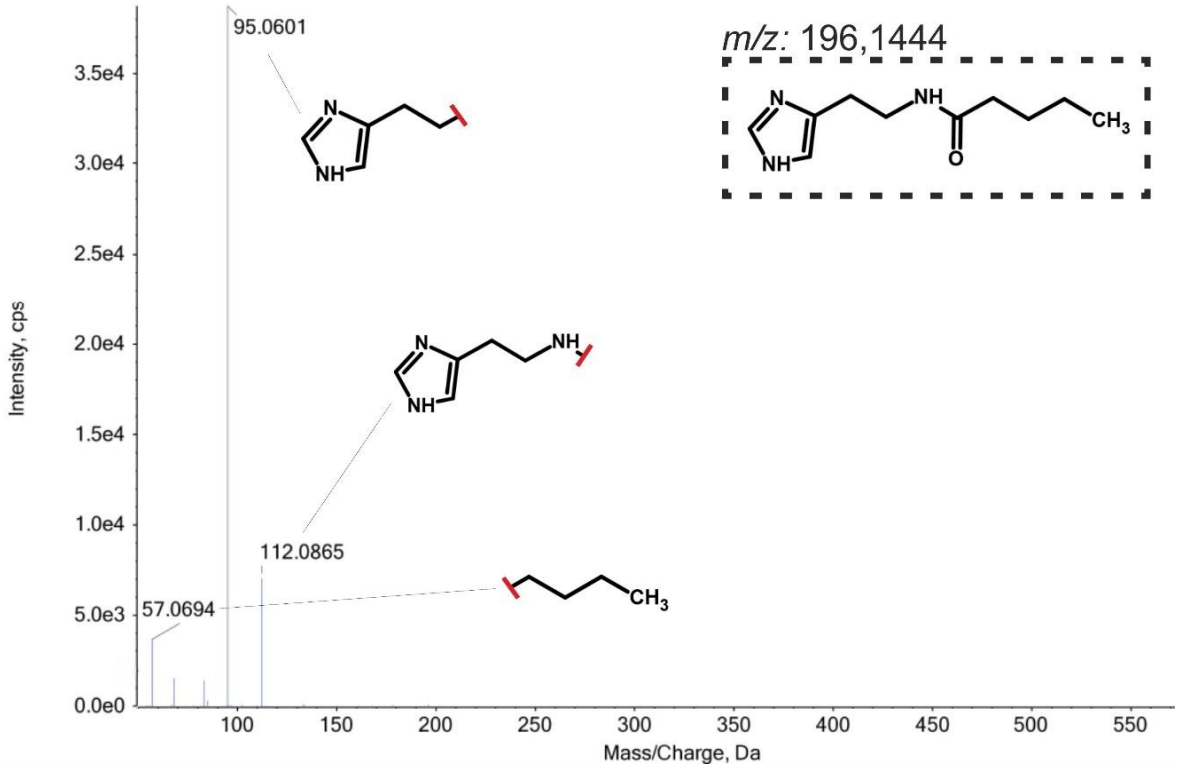

Figure 4. Positive-ion ESI-MS/MS spectrum of in-house synthesized histamine-C5:0 obtained from LC-MS/MS analysis at 1.268 min. The mass range was set at *m/z* 50–600, precursor ion was 196.1 Da and CE was 35 V. The structures of the fragment ions were annotated using Sciex OS software.

XIC obtained at *m/z* 441.38 with LC-MS analysis of the in-house Arg-C18:0 showed a clear peak at 12.261 min with -1.9 ppm mass error (Fig. 5). XIC from the Dorrestein standards mixture showed a more intense peak at 12.291 with -0.9 ppm mass error, but with additional peaks that were observed at 11.851, 13.444 and 13.952 min, with mass errors of 16.2, -26.9 and -26.7 ppm, respectively. Arg-C18:0 ion fragmentation profile matched with the Dorrestein standard mixture, with the most intense signal corresponding to the *m/z* of the precursor ion (Fig. A1). Standard mixture exhibited overall more intense fragment peaks than the in-house synthetized product. The fragments were structurally annotated using Sciex OS software's fragment ion prediction tool, utilizing mol-files that contained the structure of the Arg-C18:0 (Fig. 6). The most intense peak was confirmed as the intact precursor ion. The other peaks were significantly less intense, with the larger fragments containing the intact 18-carbon acyl tail which the smaller fragments lacked.

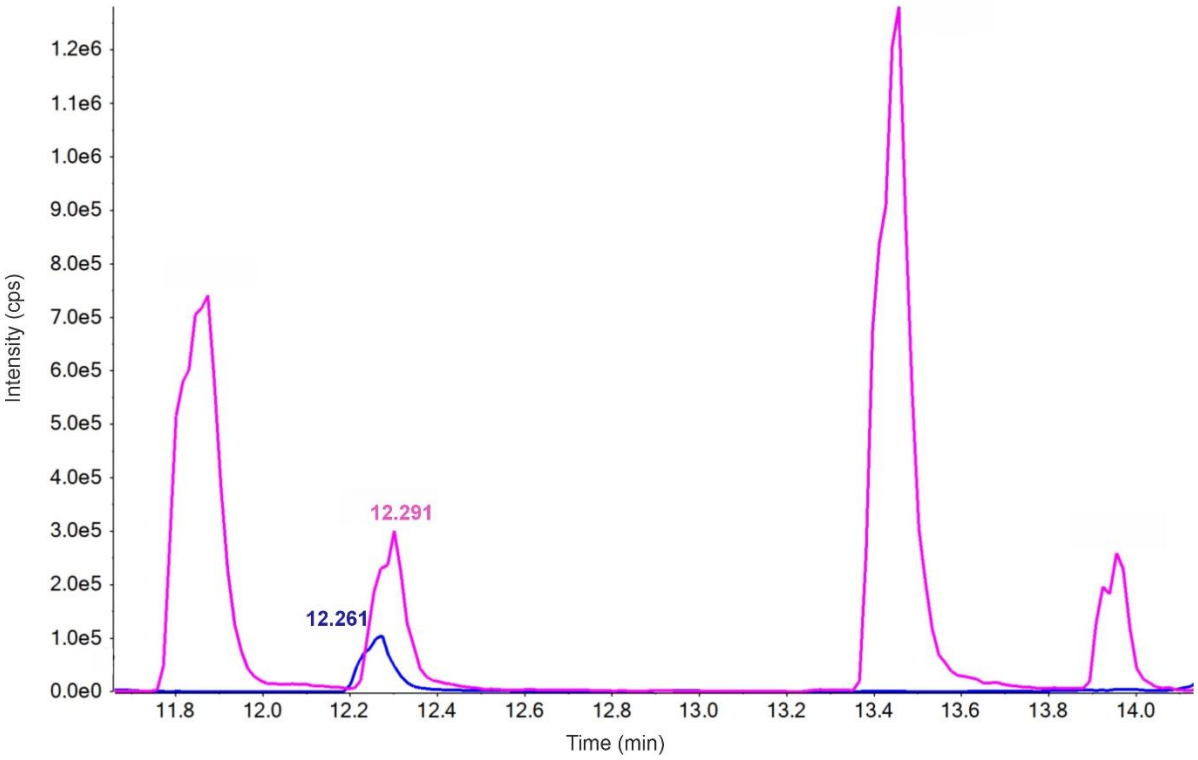

Figure 5. XIC of in-house (blue) and standard mixture (pink) Arg-C18:0 at *m/z* 441.38 obtained with LC-MS analysis. Reverse-phase C18 column (Phenomenex Kinetex 1.7 µm 100 x 2.1 mm XB-C18 100 Å column with Phenomenex SecurityGuard ULTRA Cartige pre-column) was used in UPLC separation.

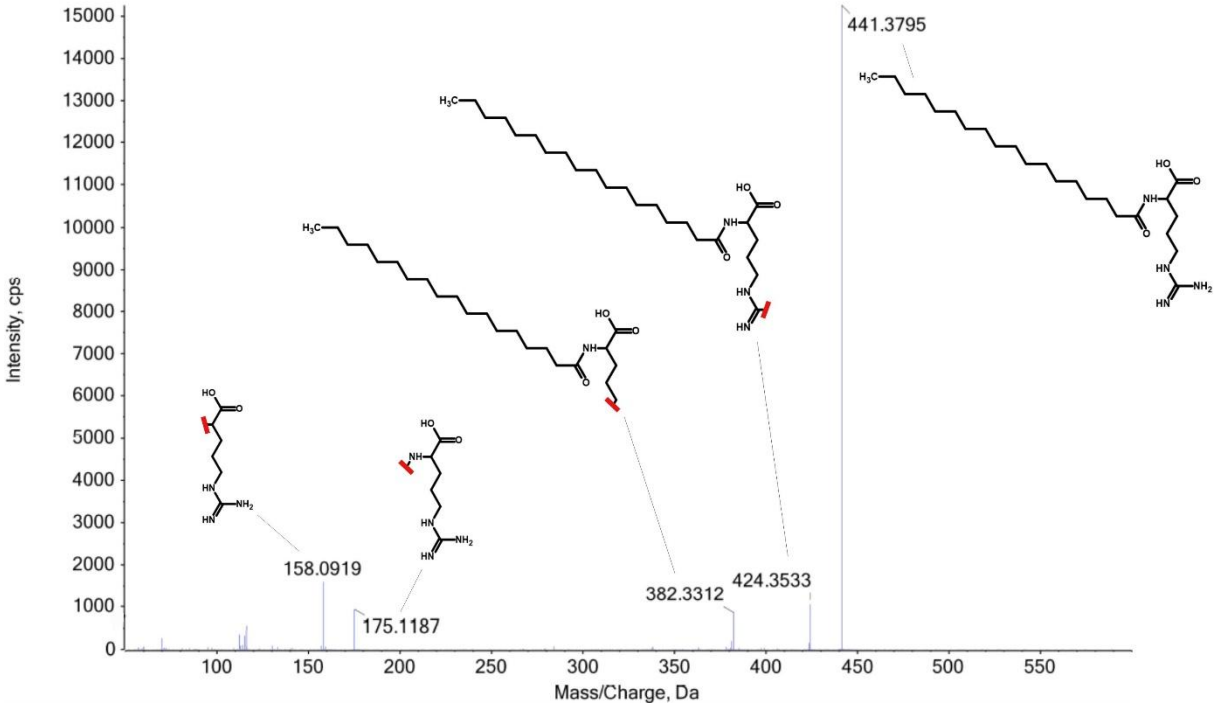

Figure 6. Positive-ion ESI-MS/MS spectrum of in-house synthetized Arg-C18:0 obtained from LC-MS/MS analysis at 12.235 min. The mass range was set at *m/z* 50–600, the precursor ion was 441.4 Da and the collision energy (CE) was 35 V. The structures of the fragment ions were annotated using Sciex OS software.

3.1.2 Nuclear resonance spectroscopy analysis

To further confirm the structures of the synthesized compounds, NMR spectroscopy analysis was conducted. ^{1}H NMR spectra was obtained to characterize the hydrogen environments in the molecules (Figs. 7 and 8), while the exact structures were confirmed with 2D NMR correlation spectroscopy (Figs. A2 and A3). Despite deviations in the ^{1}H NMR spectra from the expected proton integrations the overall pattern was correct for both of the compounds. 2D NMR correlation spectroscopy analysis verified the identification of both histamine-C5:0 and Arg-C18:0 and that there were no other isomers present. Additional peaks were detected in both synthetized standards, indicating the presence of impurities. Solvent peaks for methanol-d4 were observed approximately at their expected positions 3.31 and 4.78 ppm. Chloroform-d peak was shifted by about 0.5 ppm higher from the expected 7.24 ppm (Fig. 8).

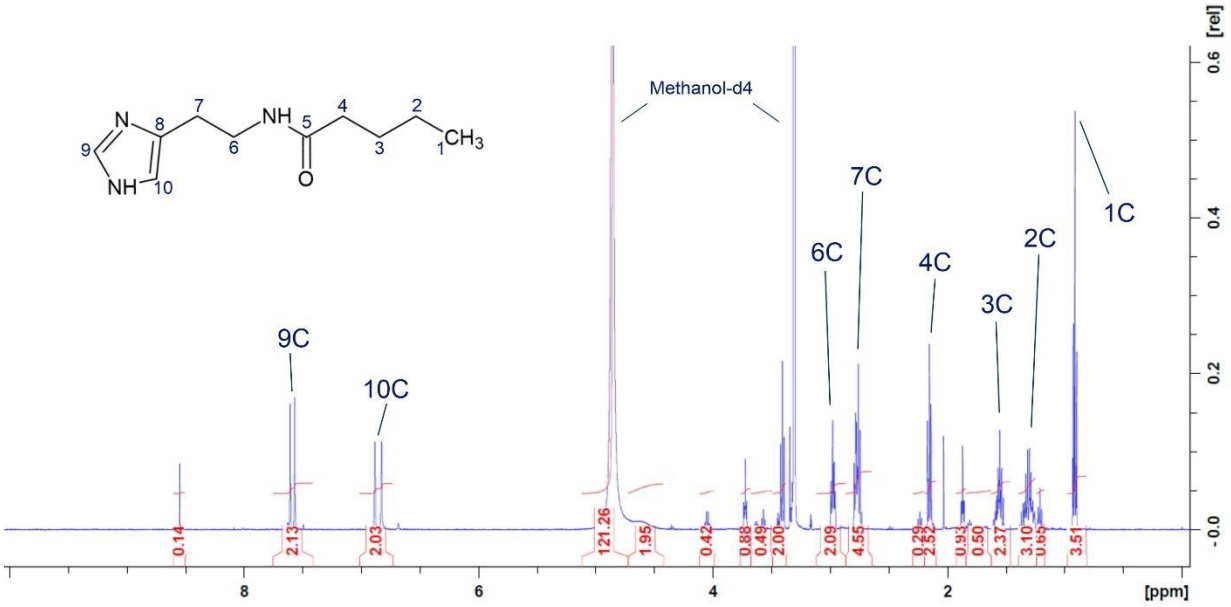

Figure 7. 500 MHz ^{1}H NMR spectrum of histamine-C5:0 in methanol-d4 solution. The structure was confirmed with 2D NMR correlation spectroscopy (Fig. A2).

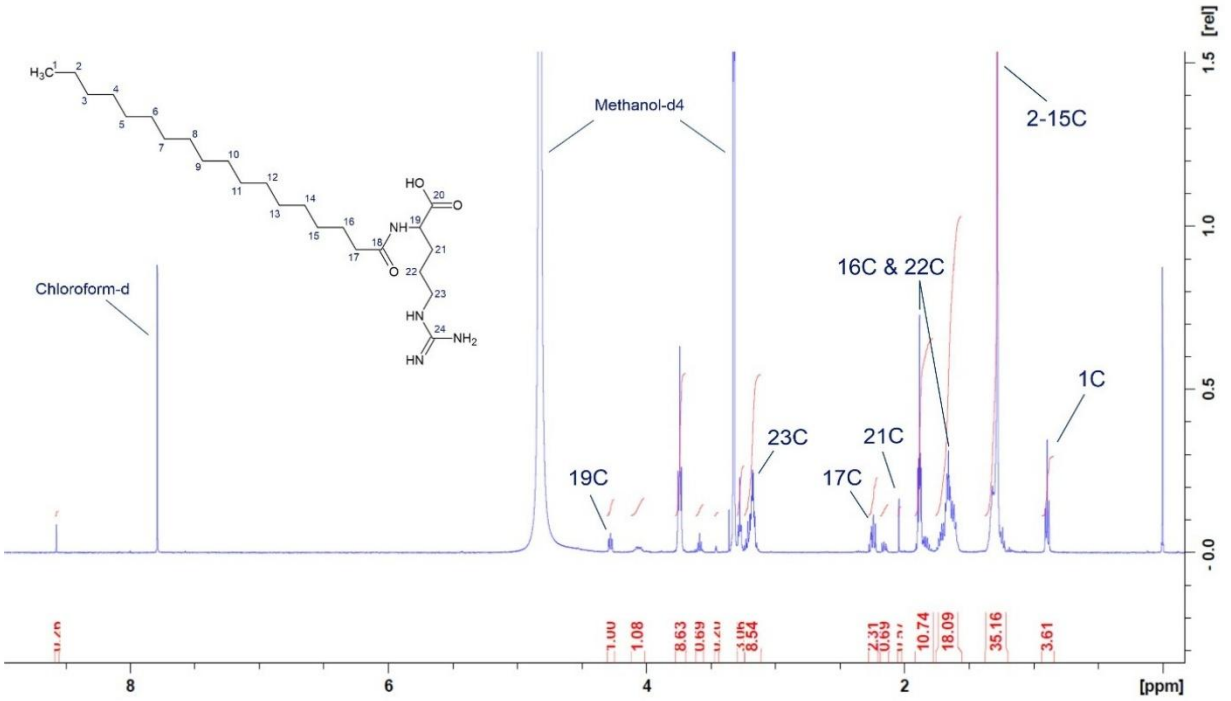

Figure 8. 500 MHz ^{1}H NMR spectrum of Arg-C18:0 in methanol-d4 and chloroform-d solution. The structure was confirmed with 2D NMR correlation spectroscopy (Fig. A3).

3.2 Method validation with quality control samples

To investigate whether the newly synthesized standards could be used in the developed targeted sMRM analysis, pooled QC samples prepared from aliquots of the main faecal samples were first analysed. Targeted sMRM analysis was set to identify each NAA by specific precursor to product ion transition in a limited retention time window. To verify the reliability of the in-house standards, they were compared against the Dorrestein NAA standard mixtures. The retention times matched between the two standards with both of the targeted NAAs (Fig. 9). Although the standards had similar peak shapes, Dorrestein standards were significantly more intense. Precursor mass errors did not exceed ± 1.1 ppm and fragment mass errors were within ± 4 ppm. The histamine-C5:0 peak detected in the QC closely resembled the shape of the standard peaks with lower intensity and a minor shift in the retention time. The QC histamine-C5:0 peak had mass error of 8.0 ppm and fragment error of -4.8 ppm. Arg-C18:0 peak detected from the QC exhibited irregular and wide shape in comparison to the standards, with precursor mass error of -6.1 ppm and fragment mass error of -0.9 ppm. The peak intensity was low but still detectable, exceeding the 3:1 signal to noise ratio, which was defined as the minimum threshold for reliable detection.

A total of 48 NAAs were targeted with the developed sMRM method with the Dorrestein standard mixtures. 33 NAAs were detected in the QC samples with precursor mass error within ± 10 ppm (Table A2). The detection included NAA isomers with different retention times which are separated from each other in the tables A1 and A2.

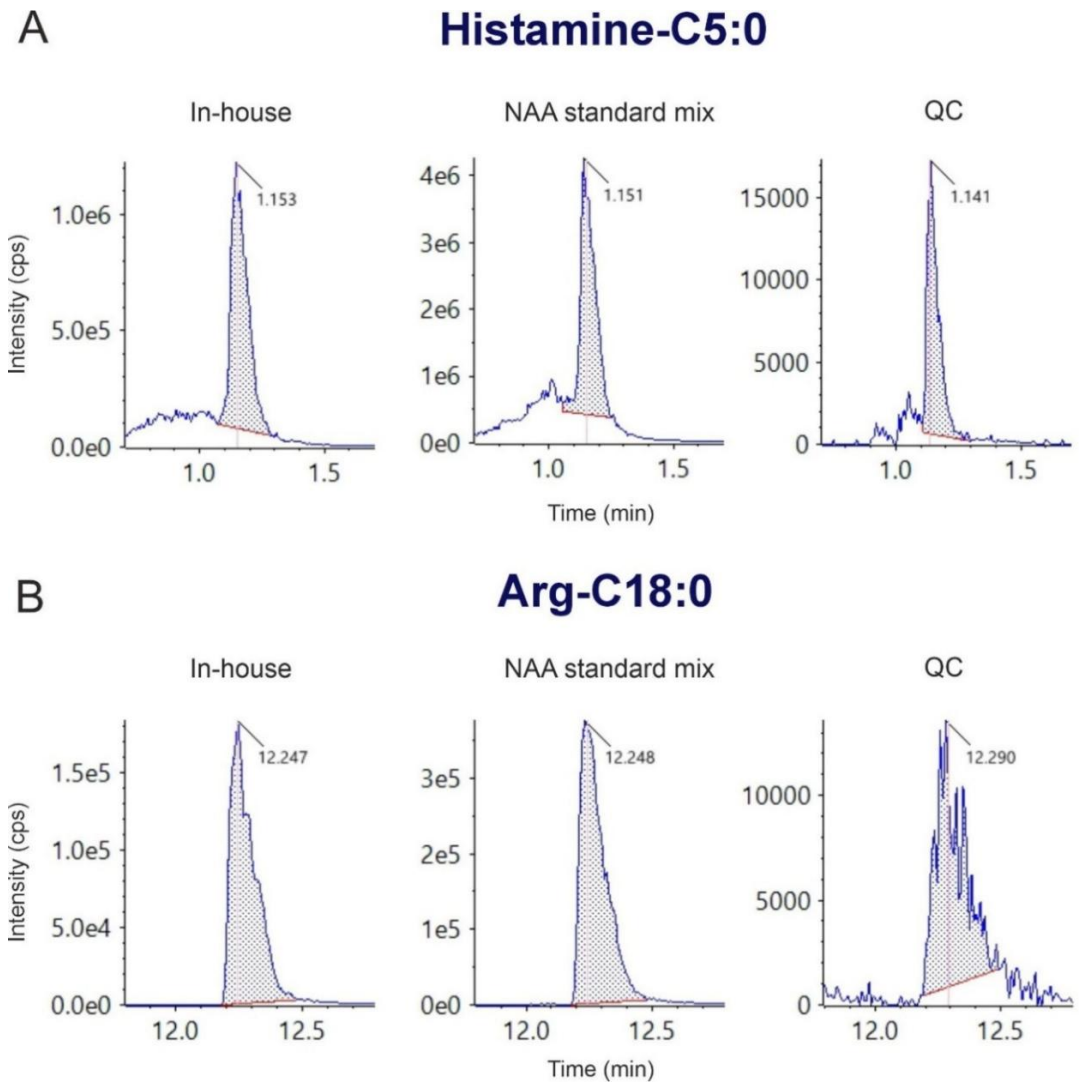

Figure 9. sMRM LC-MS/MS detection of A) histamine-C5:0 and B) Arg-C18:0 from in-house synthesized NAAs, Dorrestein NAA standard mixture and pooled QC faecal samples prepared from aliquots of the main samples.

3.3 N-acyl amide detection with targeted mass spectrometry in faecal samples

The developed sMRM method was applied in detection of the 48 NAAs (Table A1) in 40 human faecal samples, with cohort consisting of 5.5-year-olds with equal representation of both sexes. One sample was excluded from the analysis due to consistent and significant outlier values expressed across several NAAs.

Out of the 48 targeted NAAs, 32 were detected (Fig. 10). NAAs identified from the samples were verified with in-house and Dorrestein standards (Fig. 10). The most detected NAAs were tyrosine, lysine and leucine conjugates. Histamine conjugates were detected approximately in

half of the samples. Histamine-C5:0 was the most detected histamine conjugate. Arginines coupled with short chain fatty acids were detected significantly better than the long chained. Amylamine, ornithine, and putrescine conjugates were not detected.

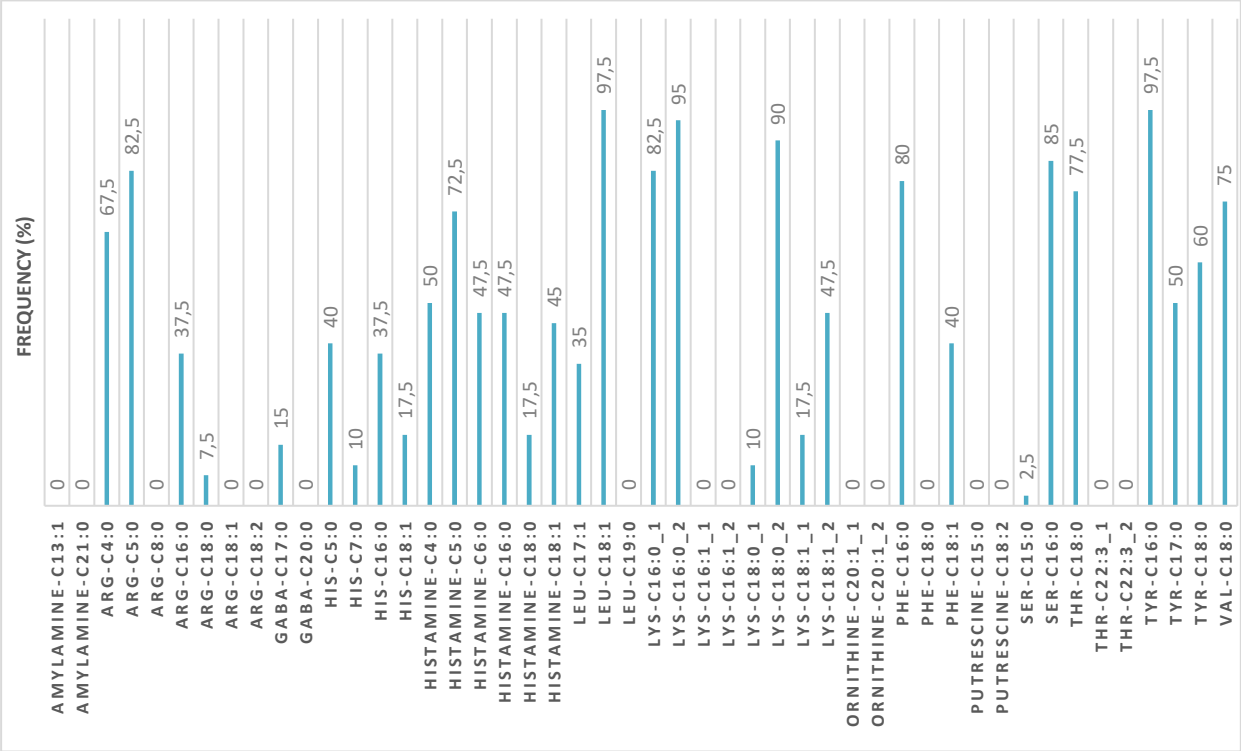

Figure 10. NAA detection frequencies (%) in human faecal samples of 5.5-year-olds obtained with targeted sMRM method. Detection frequency describes the percentage of samples NAA was detected. Out of 40 samples one was excluded due to significant outlier values across several NAAs.

29 of the NAAs detected in faecal samples were also detected earlier in the pooled QC samples (Fig. 11). His-C7:0, histamine-C6:0 and Lys-C18:1_2, were only detected in the original faecal samples whereas Arg-C8:0, Arg-C18:0, Phe-C18:0 and putrescine-C18:2, were only detected in the QC samples. Neither analysis detected any of the amylamine or ornithine conjugates. Additionally, Arg-C18:2, GABA-C20:0 and Leu-C19:0 as well as isomers of Lys-C16:1 and Thr-C22:3 went undetected in both analyses.

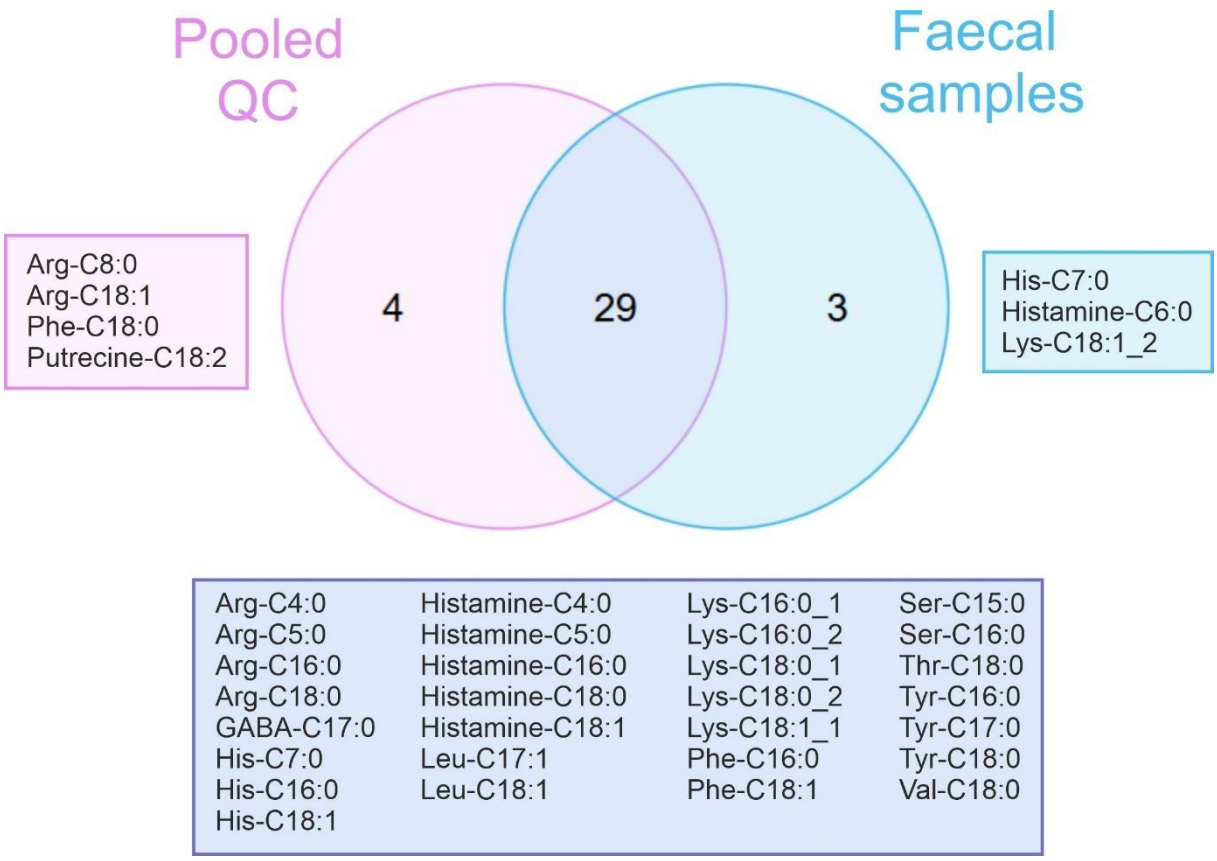

Figure 11. Venn diagram presenting NAAs detected in pooled QC and faecal samples, with the intersection displaying NAAs detected in both.

Out of the 32 detected NAAs, 27 were detected more than three times in each sex. The relative abundances of these 27 NAAs were visualized in boxplots to compare distributions between sexes (Fig. 12). Relative abundances were normalized with the internal standard aLEA-d4 to allow comparison across samples. Leu-C18:1 showed the highest relative abundance among other NAAs, followed by Lys-C16:0_2. The least abundant NAA was GABA-C17:0. Statistically significant differences in NAA abundances between sexes were not found.

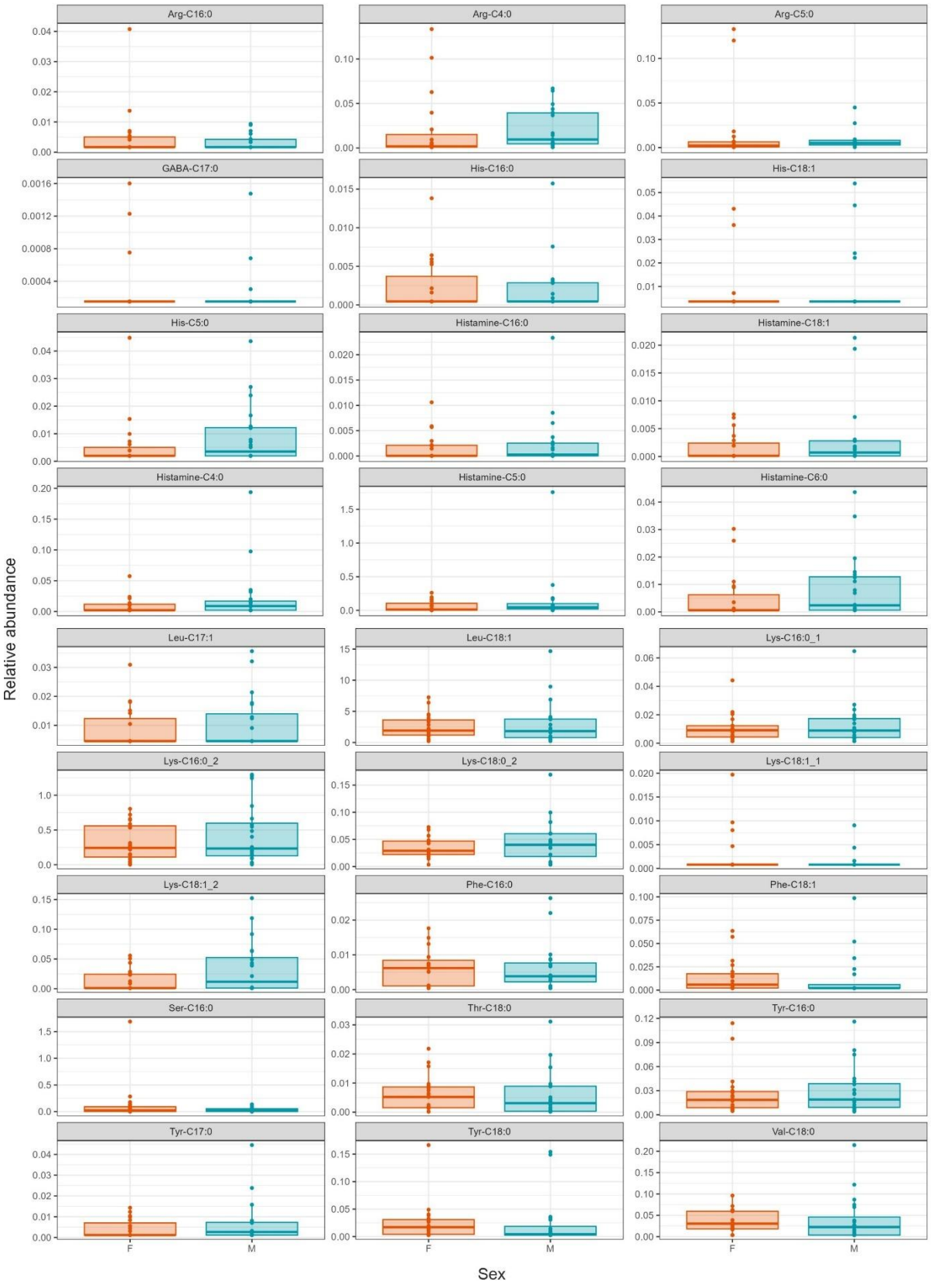

Figure 12. Boxplot comparison of NAAs detected from faecal samples between sexes. The Mann–Whitney U test showed no statistically significant differences between the groups ($p > 0.05$). Relative abundances were normalized using internal standard aLEA-d4. F: female, M: male.

4 Discussion

4.1 Evaluation of the newly synthesized N-acyl amide standards

Histamine-C5:0 and Arg-C18:0, were chosen for the chemical synthesis because they had been identified in biological samples in an earlier reverse metabolomics study (Gentry et al., 2024). Additionally, the two compounds were chosen for their structural differences. The results show that the synthesis of both, the short and long chained NAAs, was successful. LC-MS/MS analysis demonstrated matching chromatographic peaks and fragment ions between the in-house synthesized and Dorrestein standard mixture NAAs. The ion fragmentation profile of Arg-C18:0 shows that the CE was not ideal as it resulted in intense precursor peak and only little fragmentation. Therefore, in future analysis higher CE could be used in fragmentation of Arg-C18:0. In-house Arg-C18:0 exhibited one well-resolved peak in XIC, whereas in the Dorrestein standard additional peaks were observed. Difference between the chromatograms is probably due to the different synthesis strategies. In-house Arg-C18:0 was synthesized with only its precursors present in the reaction mixture resulting in interference-free chromatogram. Dorrestein standard mixtures were produced by combinatorial reaction strategy where multiple precursors react in one reaction mixture producing multiple NAAs. This approach yields numerous synthetic NAAs simultaneously and fast, but there is a higher possibility for interfering compounds in the analysis. Each of the standard mixtures utilized in this study consisted of over 450 detected NAAs, thereby increasing the possibility of detecting different product NAAs in the same XIC. Histamine-C5:0 XICs were matching between the standards with peak splitting observed in both of them. The ion fragmentation profiles of each peak were nearly identical, suggesting that the peaks represented the same compound with no additional impurities. Due to too high CE, there was no precursor ion detected in the fragment profiles, indicating that for the future measurements lower CE could be more suitable.

NMR analysis was applied to further confirm that the synthesized NAAs were authentic and could be used as qualitative standards. The expected chemical shift regions for both of the NAAs were observed in the ^{1}H NMR spectrums and the correct structures were further verified with the 2D NMR correlation spectroscopy. However, ^{1}H NMR spectrums of histamine-C5:0 and Arg-C18:0 both showed differences in the proton integration. Some peaks showed higher than expected integration values which is likely due to unreacted precursors in the non-purified mixes. For example, the proton integration value of the peak containing the carbons 2−15 in Arg-C18:0 should have a value of 28 but it shows 35 (Fig. 8). The unreacted precursor, stearic

acid, exhibits a peak at the same position which could interfere and result in a higher integration value. Histamine-C5:0 peaks exhibited less variance in the proton integration values, with the greatest difference in carbon 7 which had 2.55 higher value than expected (Fig. 7). Additional peaks were observed in spectrums of both compounds. Nevertheless, no other structures were observed from the spectrums indicating that the synthetic in-house NAAs were reliable to use as qualitative standards. These results also confirm that the LC-MS peak splitting observed with histamine-C5:0 (Fig. 3), does not represent two different compounds but is probably due to chromatographic conditions affecting the elution of histamine-C5:0. The peak splitting could be due to incomplete retention of the analyte at the column, where a portion of the injected compound does not interact with the stationary phase adequately, resulting in an early elution peak. Therefore, the later peak probably represents the actual retention time of histamine-C5:0 under these chromatographic conditions. Similar peak splitting pattern was also observed in Arg-C4:0 with sMRM LC-MS/MS method, suggesting that the high proportion of aqueous mobile phase at the start of the gradient could cause this effect specifically in short chained NAAs (Fig. A4).

4.2 Assessment of sMRM method validation

The newly developed sMRM LC-MS/MS method was first evaluated with pooled QC faecal samples to confirm its reliability before further analysis. Targeted detection of histamine-C5:0 and Arg-C18:0 demonstrated that the in-house standards were consistent with the Dorrestein standards, exhibiting similar peak shape and retention times (Fig. 9). Low mass errors detected from the standards indicate high mass accuracy of the method and the reliability of the standards. Signal intensity was lower in both in-house standards when compared to the Dorrestein standards, but still significantly higher than in the QCs. Signal intensity could be matched between the standards by adjusting the in-house standard dilutions in the future. However, both in-house and Dorrestein standards produced adequate signal for qualitative NAA detection from QC samples with the sMRM method. 33 out of the targeted 48 NAAs were detected in the QCs. These 48 NAAs were chosen specifically because they had been identified from a prior faecal analysis dataset acquired using untargeted data-dependent acquisition. Histamine-C5:0 signal from the QC samples were similar to the ones in standards, with lower intensity and higher mass error (Fig. 9). Arg-C18:0 signal from the QCs also exhibited lower intensity and higher mass error when compared to the standards. However, the peak displayed wide and irregular shape which probably resulted in slightly shifted retention time. The higher mass errors in QC samples were expected due to the biological complexity of the faeces as

matrix. Matches were considered reliable if the precursor mass error was within ± 10 ppm, signal to noise ratio was at least 3:1 and retention time differences from standard was within 0.18 min. Since Arg-C18:0 met these requirements, it was considered detected in the QC samples. The initial testing on QC samples demonstrated that the method produced reliable and consistent results. Therefore, the newly developed method with the standards were deemed ready for the analysis of the actual faecal samples.

4.3 sMRM-detected faecal N-acyl amides show no sex-related differences in relative abundances

Total of 40 faecal samples from cohort consisting of 5.5-year-olds, with equal representation of both sexes, were analysed with the developed sMRM method. Out of the 48 targeted NAAs, 32 were detected (Fig. 10). The number of detected NAAs in faecal samples reflect the number of NAAs detected in QC analysis. However, the analyses had small differences in which NAAs were detected (Fig. 11). In total, 36 NAAs were detected across both analyses, of which 26 were also reported by Gentry et al. (2024). The most frequently detected NAAs in the faecal samples consisted of leucine, lysine, tyrosine and serine conjugates. However, these groups also include NAAs that were not detected in any samples, suggesting that detection frequency is not directly consequential to the headgroup. Leu-C18:1 was one of the most frequently detected NAAs as well as the most relatively abundant one (Figs.10 and 12). This finding is consistent with Gentry et al. (2024) which identified Leu-C18:1 as one of the most frequently detected NAAs in public untargeted datasets and leucine conjugates especially frequently detected in faeces. This was also observed for other frequently detected NAAs, such as Lys-C16:0, Tyr-C16:0 and Phe-C16:0. Each of the NAAs with histamine, histidine and tyrosine amine headgroups were detected from the faecal samples. Notably, only a few histamine conjugates, C5:0, C8:0 and C20:4, were detected in the public datasets by Gentry et al. (2024). Thus, the newly developed sMRM method was capable of detecting more histamine conjugates than expected from the reverse metabolomics study. Moreover, these results indicate that the method could detect both, short and long acyl tail NAAs. Especially with arginine conjugates the short-chain conjugates were detected more frequently than the long-chain. Among histidine and histamine conjugates, there were no significant differences between the detection of long- and short-chain NAAs. Differences in detection frequencies between the NAAs may be influenced by several factors, including the stability of each compound, processing method as well as the detection limit of the MS instrument. Subsequent research examining whether different sample preparation methods influence which NAAs are detected would provide valuable information.

Additionally, increasing the cohort size could enable the detection of the NAAs unidentified in this cohort. Therefore, these results are indicative of the microbiome-derived NAA profile of the 5.5-year-olds.

Relative abundance comparison of the detected NAAs revealed no statistically significant differences between the sexes. Current research on age- and sex-related differences in faecal NAAs is limited. However, research on NAE levels in human serum does exist that examines these differences. For instance, our findings are consistent with an earlier study that detected NAEs from serum across human lifespan (Amir Hamzah et al., 2023). They found that AEA, OEA and PEA levels in age group consisting of 5−15-year-olds had minimal or no differences in the serum concentrations. Their results demonstrated that sex-dimorphism in serum NAE levels emerged later in life, with males generally exhibiting higher concentrations. Another study also found that plasma NAE levels were similar between females and males aged 18−78 (Fanelli et al., 2012). Nevertheless, these observations cannot be directly used to confirm the results obtained in this study. The NAEs detected from the serum represent metabolically distinct system from the faecal NAA profile, which is altered by the gut microbiome and the GI tract. Further research is required to determine microbiome-derived NAA profiles across sexes and age groups. Additionally, larger cohorts should be investigated to confirm the absence of sex-dependent differences.

5 Conclusions

NAAs have received a lot of interest as endogenous cell signalling molecules in the last decades. The relatively new perspective of gut microbiome communicating via self-synthesized NAAs has emerged alongside it, implying a system where the microbiome could influence its hosts physiology through gut-brain signalling. To investigate the intricate network of NAA signalling, influenced both by the host and the microbiome, authentic standards as well as robust and optimized detection methods are foundational for future research. This thesis aimed to address these gaps in microbiome-derived NAA research. Chemical synthesis and characterization of novel NAA standards offered reliable qualitative standards for the LC-MS/MS analysis. The chemical synthesis plan presented here could be applied to synthesize more individual NAA standards. Furthermore, developing a purification protocol for the newly synthesized compounds would allow applying them to quantitative research in the future, which would provide even more detailed information about the NAA profiles. The developed targeted LC-MS/MS analysis method identified majority of the NAAs, demonstrating its utility in the detection in faecal samples, which remain underexplored due to their biological complexity. Since NAAs are a group with substantial structural diversity, the sMRM method could be extended to measure even wider NAA profiles in the future. Overall, this approach improves the detection and understanding of gut microbiome-derived NAAs in human physiology. Applied to larger cohorts it could uncover how gut microbiome-derived NAA profiles are shaped by different factors, such as age, lifestyle and diseases.

References

Akanmu, M., Adeosun, S., & Ilesanmi, O. (2007). Neuropharmacological effects of oleamide in male and female mice. *Behavioural Brain Research*, *182*(1), 88–94. https://doi.org/10.1016/j.bbr.2007.05.006

Alawi, K., & Keeble, J. (2010). The paradoxical role of the transient receptor potential vanilloid 1 receptor in inflammation. *Pharmacology & Therapeutics*, *125*(2), 181–195. https://doi.org/10.1016/j.pharmthera.2009.10.005

Ameri, A., Wilhelm, A., & Simmet, T. (1999). Effects of the endogeneous cannabinoid, anandamide, on neuronal activity in rat hippocampal slices. *British Journal of Pharmacology*, *126*(8), 1831–1839. https://doi.org/10.1038/sj.bjp.0702478

Amir Hamzah, K., Toms, L.-M., Kucharski, N., Orr, J., Turner, N. P., Hobson, P., Nichols, D. S., & Ney, L. J. (2023). Sex-dimorphism in human serum endocannabinoid and n-acyl ethanolamine concentrations across the lifespan. *Scientific Reports*, *13*(1), 23059. https://doi.org/10.1038/s41598-023-50426-4

Amir Hamzah, K., Turner, N., Nichols, D., & Ney, L. J. (2025). Advances in targeted liquid chromatography-tandem mass spectrometry methods for endocannabinoid and N-acylethanolamine quantification in biological matrices: A systematic review. *Mass Spectrometry Reviews*, *44*(3), 513–538. https://doi.org/10.1002/mas.21897

Arafat, E. S., Trimble, J. W., Andersen, R. N., Dass, C., & Desiderio, D. M. (1989). Identification of fatty acid amides in human plasma. *Life Sciences*, *45*(18), 1679–1687. https://doi.org/10.1016/0024-3205(89)90278-6

Artmann, A., Petersen, G., Hellgren, L. I., Boberg, J., Skonberg, C., Nellemann, C., Hansen, S. H., & Hansen, H. S. (2008). Influence of dietary fatty acids on endocannabinoid and N-acylethanolamine levels in rat brain, liver and small intestine. *Biochimica et Biophysica Acta (BBA) - Molecular and Cell Biology of Lipids*, *1781*(4), 200–212. https://doi.org/10.1016/j.bbalip.2008.01.006

Bennion, D., Jensen, T., Walther, C., Hamblin, J., Wallmann, A., Couch, J., Blickenstaff, J., Castle, M., Dean, L., Beckstead, S., Merrill, C., Muir, C., St. Pierre, T., Williams, B., Daniel, S., & Edwards, J. G. (2011). Transient receptor potential vanilloid 1 agonists modulate hippocampal CA1 LTP via the GABAergic system. *Neuropharmacology*, *61*(4), 730–738. https://doi.org/10.1016/j.neuropharm.2011.05.018

Berland, C., Castel, J., Terrasi, R., Montalban, E., Foppen, E., Martin, C., Muccioli, G. G., Luquet, S., & Gangarossa, G. (2022). Identification of an endocannabinoid gut-brain vagal mechanism controlling food reward and energy homeostasis. *Molecular Psychiatry*, *27*(4), 2340–2354. https://doi.org/10.1038/s41380-021-01428-z

Bisogno, T., Melck, D., Bobrov, M. Y., Gretskaya, N. M., Bezuglov, V. V., Petrocellis, L. D., & Marzo, V. D. (2000). *N-acyl-dopamines: Novel synthetic CB1 cannabinoid-receptor ligands and inhibitors of anandamide inactivation with cannabimimetic activity in vitro and in vivo*.

Bondarenko, A. I., Drachuk, K., Panasiuk, O., Sagach, V., Deak, A. T., Malli, R., & Graier, W. F. (2013). N-arachidonoyl glycine suppresses Na+/Ca2+ exchanger-mediated Ca2+ entry into endothelial cells and activates BKCa channels independently of GPCRs. *British Journal of Pharmacology*, *169*(4), 933–948. https://doi.org/10.1111/bph.12180

Bouaboula, M., Hilairet, S., Marchand, J., Fajas, L., Fur, G. L., & Casellas, P. (2005). Anandamide induced PPARγ transcriptional activation and 3T3-L1 preadipocyte differentiation. *European Journal of Pharmacology*, *517*(3), 174–181. https://doi.org/10.1016/j.ejphar.2005.05.032

Bradshaw, H. B., Rimmerman, N., Hu, S.-J., Benton, V. M., Stuart, J. M., Masuda, K., Cravatt, B. F., O'Dell, D. K., & Walker, J. M. (2009). The endocannabinoid anandamide is a precursor for the signaling lipid N-arachidonoyl glycine by two distinct pathways. *BMC Biochemistry*, *10*(1). Scopus. https://doi.org/10.1186/1471-2091-10-14

Bradshaw, H. B., & Walker, J. M. (2005). The expanding field of cannabimimetic and related lipid mediators. *British Journal of Pharmacology*, *144*(4), 459–465. https://doi.org/10.1038/sj.bjp.0706093

Burstein, S. H., Adams, J. K., Bradshaw, H. B., Fraioli, C., Rossetti, R. G., Salmonsen, R. A., Shaw, J. W., Walker, J. M., Zipkin, R. E., & Zurier, R. B. (2007). Potential anti-inflammatory actions

of the elmiric (lipoamino) acids. *Bioorganic & Medicinal Chemistry*, *15*(10), 3345–3355. https://doi.org/10.1016/j.bmc.2007.03.026

Burstein, S., & Salmonsen, R. (2008). Acylamido analogs of endocannabinoids selectively inhibit cancer cell proliferation. *Bioorganic & Medicinal Chemistry*, *16*(22), 9644–9651. https://doi.org/10.1016/j.bmc.2008.10.015

Cadas, H., Tomaso, E. di, & Piomelli, D. (1997). Occurrence and Biosynthesis of Endogenous Cannabinoid Precursor,N-Arachidonoyl Phosphatidylethanolamine, in Rat Brain. *Journal of Neuroscience*, *17*(4), 1226–1242. https://doi.org/10.1523/JNEUROSCI.17-04-01226.1997

Calignano, A., Rana, G. L., Giuffrida, A., & Piomelli, D. (1998). Control of pain initiation by endogenous cannabinoids. *Nature*, *394*(6690), 277–281. https://doi.org/10.1038/28393

Campolongo, P., Roozendaal, B., Trezza, V., Cuomo, V., Astarita, G., Fu, J., McGaugh, J. L., & Piomelli, D. (2009). Fat-induced satiety factor oleoylethanolamide enhances memory consolidation. *Proceedings of the National Academy of Sciences*, *106*(19), 8027–8031. https://doi.org/10.1073/pnas.0903038106

Cani, P. D., Plovier, H., Van Hul, M., Geurts, L., Delzenne, N. M., Druart, C., & Everard, A. (2016). Endocannabinoids—At the crossroads between the gut microbiota and host metabolism. *Nature Reviews Endocrinology*, *12*(3), 133–143. https://doi.org/10.1038/nrendo.2015.211

Caterina, M. J., Leffler, A., Malmberg, A. B., Martin, W. J., Trafton, J., Petersen-Zeitz, K. R., Koltzenburg, M., Basbaum, A. I., & Julius, D. (2000). Impaired Nociception and Pain Sensation in Mice Lacking the Capsaicin Receptor. *Science*, *288*(5464), 306–313. https://doi.org/10.1126/science.288.5464.306

Centonze, D., Bari, M., Rossi, S., Prosperetti, C., Furlan, R., Fezza, F., De Chiara, V., Battistini, L., Bernardi, G., Bernardini, S., Martino, G., & Maccarrone, M. (2007). The endocannabinoid system is dysregulated in multiple sclerosis and in experimental autoimmune encephalomyelitis. *Brain*, *130*(10), 2543–2553. https://doi.org/10.1093/brain/awm160

Chevalier, G., Siopi, E., Guenin-Macé, L., Pascal, M., Laval, T., Rifflet, A., Boneca, I. G., Demangel, C., Colsch, B., Pruvost, A., Chu-Van, E., Messager, A., Leulier, F., Lepousez, G., Eberl, G., & Lledo, P.-M. (2020). Effect of gut microbiota on depressive-like behaviors in mice is mediated

by the endocannabinoid system. *Nature Communications*, *11*(1), 6363. https://doi.org/10.1038/s41467-020-19931-2

Chiurchiù, V., van der Stelt, M., Centonze, D., & Maccarrone, M. (2018). The endocannabinoid system and its therapeutic exploitation in multiple sclerosis: Clues for other neuroinflammatory diseases. *Progress in Neurobiology*, *160*, 82–100. https://doi.org/10.1016/j.pneurobio.2017.10.007

Chu, C. J., Huang, S. M., Petrocellis, L. D., Bisogno, T., Ewing, S. A., Miller, J. D., Zipkin, R. E., Daddario, N., Appendino, G., Marzo, V. D., & Walker, J. M. (2003). N-Oleoyldopamine, a Novel Endogenous Capsaicin-like Lipid That Produces Hyperalgesia *. *Journal of Biological Chemistry*, *278*(16), 13633–13639. https://doi.org/10.1074/jbc.M211231200

Cohen, L. J., Esterhazy, D., Kim, S.-H., Lemetre, C., Aguilar, R. R., Gordon, E. A., Pickard, A. J., Cross, J. R., Emiliano, A. B., Han, S. M., Chu, J., Vila-Farres, X., Kaplitt, J., Rogoz, A., Calle, P. Y., Hunter, C., Bitok, J. K., & Brady, S. F. (2017). Commensal bacteria make GPCR ligands that mimic human signalling molecules. *Nature*, *549*(7670), 48–53. https://doi.org/10.1038/nature23874

Console-Bram, L., Ciuciu, S. M., Zhao, P., Zipkin, R. E., Brailoiu, E., & Abood, M. E. (2017). N-arachidonoyl glycine, another endogenous agonist of GPR55. *Biochemical and Biophysical Research Communications*, *490*(4), 1389–1393. https://doi.org/10.1016/j.bbrc.2017.07.038

Cravatt, B. F., Demarest, K., Patricelli, M. P., Bracey, M. H., Giang, D. K., Martin, B. R., & Lichtman, A. H. (2001). Supersensitivity to anandamide and enhanced endogenous cannabinoid signaling in mice lacking fatty acid amide hydrolase. *Proceedings of the National Academy of Sciences*, *98*(16), 9371–9376. https://doi.org/10.1073/pnas.161191698

Cravatt, B. F., Giang, D. K., Mayfield, S. P., Boger, D. L., Lerner, R. A., & Gilula, N. B. (1996). Molecular characterization of an enzyme that degrades neuromodulatory fatty-acid amides. *Nature*, *384*(6604), 83–87. https://doi.org/10.1038/384083a0

Cravatt, B. F., Prospero-Garcia, O., Siuzdak, G., Gilula, N. B., Henriksen, S. J., Boger, D. L., & Lerner, R. A. (1995). Chemical Characterization of a Family of Brain Lipids That Induce Sleep. *Science*, *268*(5216), 1506–1509. https://doi.org/10.1126/science.7770779

Cristino, L., Bisogno, T., & Di Marzo, V. (2020). Cannabinoids and the expanded endocannabinoid system in neurological disorders. *Nature Reviews Neurology*, *16*(1), 9–29. https://doi.org/10.1038/s41582-019-0284-z

Cuddihey, H., Cavin, J.-B., Keenan, C. M., Wallace, L. E., Vemuri, K., Makriyannis, A., MacNaughton, W. K., & Sharkey, K. A. (2022). Role of CB1 receptors in the acute regulation of small intestinal permeability: Effects of high-fat diet. *American Journal of Physiology-Gastrointestinal and Liver Physiology*, *323*(3), G219–G238. https://doi.org/10.1152/ajpgi.00341.2021

Dalle Carbonare, M., Del Giudice, E., Stecca, A., Colavito, D., Fabris, M., D'Arrigo, A., Bernardini, D., Dam, M., & Leon, A. (2008). A Saturated N-Acylethanolamine Other than N-Palmitoyl Ethanolamine with Anti-inflammatory Properties: A Neglected Story…. *Journal of Neuroendocrinology*, *20*(s1), 26–34. https://doi.org/10.1111/j.1365-2826.2008.01689.x

Darré, L., & Domene, C. (2015). Binding of Capsaicin to the TRPV1 Ion Channel. *Molecular Pharmaceutics*, *12*(12), 4454–4465. https://doi.org/10.1021/acs.molpharmaceut.5b00641

De Petrocellis, L., Bisogno, T., Maccarrone, M., Davis, J. B., Finazzi-Agrò, A., & Di Marzo, V. (2001). The Activity of Anandamide at Vanilloid VR1 Receptors Requires Facilitated Transport across the Cell Membrane and Is Limited by Intracellular Metabolism. *Journal of Biological Chemistry*, *276*(16), 12856–12863. https://doi.org/10.1074/jbc.M008555200

De Petrocellis, L., Chu, C. J., Moriello, A. S., Kellner, J. C., Walker, J. M., & Di Marzo, V. (2004). Actions of two naturally occurring saturated N-acyldopamines on transient receptor potential vanilloid 1 (TRPV1) channels. *British Journal of Pharmacology*, *143*(2), 251–256. https://doi.org/10.1038/sj.bjp.0705924

De Petrocellis, L., Starowicz, K., Moriello, A. S., Vivese, M., Orlando, P., & Di Marzo, V. (2007). Regulation of transient receptor potential channels of melastatin type 8 (TRPM8): Effect of cAMP, cannabinoid CB1 receptors and endovanilloids. *Experimental Cell Research*, *313*(9), 1911–1920. https://doi.org/10.1016/j.yexcr.2007.01.008

De Pol, M., & Kolla, N. J. (2021). Endocannabinoid markers in autism spectrum disorder: A scoping review of human studies. *Psychiatry Research*, *306*, 114256. https://doi.org/10.1016/j.psychres.2021.114256

Deda, O., Gika, H. G., Wilson, I. D., & Theodoridis, G. A. (2015). An overview of fecal sample preparation for global metabolic profiling. *Journal of Pharmaceutical and Biomedical Analysis, REVIEW 2015*, *113*, 137–150. https://doi.org/10.1016/j.jpba.2015.02.006

Devane, W. A., Dysarz, F. A., Johnson, M. R., Melvin, L. S., & Howlett, A. C. (1988). Determination and characterization of a cannabinoid receptor in rat brain. *Molecular Pharmacology*, *34*(5), 605–613. https://doi.org/10.1016/S0026-895X(25)09876-1

Devane, W. A., Hanuš, L., Breuer, A., Pertwee, R. G., Stevenson, L. A., Griffin, G., Gibson, D., Mandelbaum, A., Etinger, A., & Mechoulam, R. (1992). Isolation and Structure of a Brain Constituent That Binds to the Cannabinoid Receptor. *Science*, *258*, 1946–1949. https://doi.org/10.1126/science.1470919

Divito, E. B., & Cascio, M. (2013). Metabolism, Physiology, and Analyses of Primary Fatty Acid Amides. *Chemical Reviews*, *113*(10), 7343–7353. https://doi.org/10.1021/cr300363b

Dlugos, A., Childs, E., Stuhr, K. L., Hillard, C. J., & Wit, H. de. (2012). Acute Stress Increases Circulating Anandamide and Other N-Acylethanolamines in Healthy Humans. *Neuropsychopharmacology*, *37*(11), 2416. https://doi.org/10.1038/npp.2012.100

Dohnalová, L., Lundgren, P., Carty, J. R. E., Goldstein, N., Wenski, S. L., Nanudorn, P., Thiengmag, S., Huang, K.-P., Litichevskiy, L., Descamps, H. C., Chellappa, K., Glassman, A., Kessler, S., Kim, J., Cox, T. O., Dmitrieva-Posocco, O., Wong, A. C., Allman, E. L., Ghosh, S., … Thaiss, C. A. (2022). A microbiome-dependent gut–brain pathway regulates motivation for exercise. *Nature*, *612*(7941), 739–747. https://doi.org/10.1038/s41586-022-05525-z

Eshawu, A. B., Gunda, T. J., Kumar, B., & Matta, S. (2025). Advancements in sample preparation and extraction techniques for metabolomic analysis of animal fluids. *Microchemical Journal*, *218*, 115259. https://doi.org/10.1016/j.microc.2025.115259

Esposito, E., Impellizzeri, D., Mazzon, E., Paterniti, I., & Cuzzocrea, S. (2012). Neuroprotective Activities of Palmitoylethanolamide in an Animal Model of Parkinson's Disease. *PLOS ONE*, *7*(8), e41880. https://doi.org/10.1371/journal.pone.0041880

Fanelli, F., Di Lallo, V. D., Belluomo, I., De Iasio, R., Baccini, M., Casadio, E., Gasparini, D. I., Colavita, M., Gambineri, A., Grossi, G., Vicennati, V., Pasquali, R., & Pagotto, U. (2012). Estimation of reference intervals of five endocannabinoids and endocannabinoid related compounds in human plasma by two dimensional-LC/MS/MS. *Journal of Lipid Research*, *53*(3), 481–493. https://doi.org/10.1194/jlr.M021378

Fontana, A., Di Marzo, V., Cadas, H., & Piomelli, D. (1995). Analysis of anandamide, an endogenous cannabinoid substance, and of other natural *N*-acylethanolamines. *Prostaglandins, Leukotrienes and Essential Fatty Acids*, *53*(4), 301–308. https://doi.org/10.1016/0952-3278(95)90130-2

Franklin, A., Parmentier-Batteur, S., Walter, L., Greenberg, D. A., & Stella, N. (2003). Palmitoylethanolamide Increases after Focal Cerebral Ischemia and Potentiates Microglial Cell Motility. *Journal of Neuroscience*, *23*(21), 7767–7775. https://doi.org/10.1523/JNEUROSCI.23-21-07767.2003

Fu, J., Gaetani, S., Oveisi, F., Lo Verme, J., Serrano, A., Rodríguez de Fonseca, F., Rosengarth, A., Luecke, H., Di Giacomo, B., Tarzia, G., & Piomelli, D. (2003). Oleylethanolamide regulates feeding and body weight through activation of the nuclear receptor PPAR-α. *Nature*, *425*(6953), 90–93. https://doi.org/10.1038/nature01921

Galiègue, S., Mary, S., Marchand, J., Dussossoy, D., Carrière, D., Carayon, P., Bouaboula, M., Shire, D., LE Fur, G., & Casellas, P. (1995). Expression of Central and Peripheral Cannabinoid Receptors in Human Immune Tissues and Leukocyte Subpopulations. *European Journal of Biochemistry*, *232*(1), 54–61. https://doi.org/10.1111/j.1432-1033.1995.tb20780.x

Gaoni, Y., & Mechoulam, R. (1964). Isolation, Structure, and Partial Synthesis of an Active Constituent of Hashish. *Journal of the American Chemical Society*, *86*(8), 1646–1647. https://doi.org/10.1021/ja01062a046

Gentry, E. C., Collins, S. L., Panitchpakdi, M., Belda-Ferre, P., Stewart, A. K., Carrillo Terrazas, M., Lu, H., Zuffa, S., Yan, T., Avila-Pacheco, J., Plichta, D. R., Aron, A. T., Wang, M., Jarmusch, A. K., Hao, F., Syrkin-Nikolau, M., Vlamakis, H., Ananthakrishnan, A. N., Boland, B. S., … Dorrestein, P. C. (2024). Reverse metabolomics for the discovery of chemical structures from humans. *Nature*, *626*(7998), 419–426. https://doi.org/10.1038/s41586-023-06906-8

Gobbi, G., Bambico, F. R., Mangieri, R., Bortolato, M., Campolongo, P., Solinas, M., Cassano, T., Morgese, M. G., Debonnel, G., Duranti, A., Tontini, A., Tarzia, G., Mor, M., Trezza, V., Goldberg, S. R., Cuomo, V., & Piomelli, D. (2005). Antidepressant-like activity and modulation of brain monoaminergic transmission by blockade of anandamide hydrolysis. *Proceedings of the National Academy of Sciences*, *102*(51), 18620–18625. https://doi.org/10.1073/pnas.0509591102

Gómez, R., Navarro, M., Ferrer, B., Trigo, J. M., Bilbao, A., Arco, I. D., Cippitelli, A., Nava, F., Piomelli, D., & Fonseca, F. R. de. (2002). A Peripheral Mechanism for CB1 Cannabinoid Receptor-Dependent Modulation of Feeding. *Journal of Neuroscience*, *22*(21), 9612–9617. https://doi.org/10.1523/JNEUROSCI.22-21-09612.2002

Gowran, A., Noonan, J., & Campbell, V. A. (2011). The Multiplicity of Action of Cannabinoids: Implications for Treating Neurodegeneration. *CNS Neuroscience & Therapeutics*, *17*(6), 637–644. https://doi.org/10.1111/j.1755-5949.2010.00195.x

Grabon, W., Ruiz, A., Gasmi, N., Degletagne, C., Georges, B., Belmeguenai, A., Bodennec, J., Rheims, S., Marcy, G., & Bezin, L. (2024). CB2 expression in mouse brain: From mapping to regulation in microglia under inflammatory conditions. *Journal of Neuroinflammation*, *21*(1), 206. https://doi.org/10.1186/s12974-024-03202-8

Graham, E. S., Angel, C. E., Schwarcz, L. E., Dunbar, P. R., & Glass, M. (2010). Detailed Characterisation of CB2 Receptor Protein Expression in Peripheral Blood Immune Cells from Healthy Human Volunteers Using Flow Cytometry. *International Journal of Immunopathology and Pharmacology*, *23*(1), 25–34. https://doi.org/10.1177/039463201002300103

Grazia Cascio, M., Minassi, A., Ligresti, A., Appendino, G., Burstein, S., & Di Marzo, V. (2004). A structure–activity relationship study on N-arachidonoyl-amino acids as possible endogenous inhibitors of fatty acid amide hydrolase. *Biochemical and Biophysical Research Communications*, *314*(1), 192–196. https://doi.org/10.1016/j.bbrc.2003.12.075

Gross, J. H. (2017). *Mass Spectrometry*. Springer International Publishing. https://doi.org/10.1007/978-3-319-54398-7

Hansen, H. S., Rosenkilde, M. M., Holst, J. J., & Schwartz, T. W. (2012). GPR119 as a fat sensor. *Trends in Pharmacological Sciences*, *33*(7), 374–381. https://doi.org/10.1016/j.tips.2012.03.014

Herkenham, M., Lynn, A. B., Little, M. D., Johnson, M. R., Melvin, L. S., de Costa, B. R., & Rice, K. C. (1990). Cannabinoid receptor localization in brain. *Proceedings of the National Academy of Sciences*, *87*(5), 1932–1936. https://doi.org/10.1073/pnas.87.5.1932

Hill, M. N., McLaughlin, R. J., Morrish, A. C., Viau, V., Floresco, S. B., Hillard, C. J., & Gorzalka, B. B. (2009). Suppression of Amygdalar Endocannabinoid Signaling by Stress Contributes to Activation of the Hypothalamic–Pituitary–Adrenal Axis. *Neuropsychopharmacology*, *34*(13), 2733–2745. https://doi.org/10.1038/npp.2009.114

Hohmann, A. G., Suplita, R. L., Bolton, N. M., Neely, M. H., Fegley, D., Mangieri, R., Krey, J. F., Michael Walker, J., Holmes, P. V., Crystal, J. D., Duranti, A., Tontini, A., Mor, M., Tarzia, G., & Piomelli, D. (2005). An endocannabinoid mechanism for stress-induced analgesia. *Nature*, *435*(7045), 1108–1112. https://doi.org/10.1038/nature03658

Huang, S. M., Bisogno, T., Petros, T. J., Chang, S. Y., Zavitsanos, P. A., Zipkin, R. E., Sivakumar, R., Coop, A., Maeda, D. Y., De Petrocellis, L., Burstein, S., Di Marzo, V., & Walker, J. M. (2001). Identification of a New Class of Molecules, the Arachidonyl Amino Acids, and Characterization of One Member That Inhibits Pain*. *Journal of Biological Chemistry*, *276*(46), 42639–42644. https://doi.org/10.1074/jbc.M107351200

Iannotti, F. A., Di Marzo, V., & Petrosino, S. (2016). Endocannabinoids and endocannabinoid-related mediators: Targets, metabolism and role in neurological disorders. *Progress in Lipid Research*, *62*, 107–128. https://doi.org/10.1016/j.plipres.2016.02.002

Iannotti, F. A., Hill, C. L., Leo, A., Alhusaini, A., Soubrane, C., Mazzarella, E., Russo, E., Whalley, B. J., Di Marzo, V., & Stephens, G. J. (2014). Nonpsychotropic Plant Cannabinoids, Cannabidivarin (CBDV) and Cannabidiol (CBD), Activate and Desensitize Transient Receptor Potential Vanilloid 1 (TRPV1) Channels in Vitro: Potential for the Treatment of Neuronal Hyperexcitability. *ACS Chemical Neuroscience*, *5*(11), 1131–1141. https://doi.org/10.1021/cn5000524

Igarashi, M., DiPatrizio, N. V., Narayanaswami, V., & Piomelli, D. (2015). Feeding-induced oleoylethanolamide mobilization is disrupted in the gut of diet-induced obese rodents. *Biochimica et Biophysica Acta (BBA) - Molecular and Cell Biology of Lipids*, *1851*(9), 1218–1226. https://doi.org/10.1016/j.bbalip.2015.05.006

Julius, D. (2013). TRP Channels and Pain. *Annual Review of Cell and Developmental Biology*, *29*(1), 355–384. https://doi.org/10.1146/annurev-cellbio-101011-155833

Karu, N., Deng, L., Slae, M., Guo, A. C., Sajed, T., Huynh, H., Wine, E., & Wishart, D. S. (2018). A review on human fecal metabolomics: Methods, applications and the human fecal metabolome database. *Analytica Chimica Acta*, *1030*, 1–24. https://doi.org/10.1016/j.aca.2018.05.031

Kathuria, S., Gaetani, S., Fegley, D., Valiño, F., Duranti, A., Tontini, A., Mor, M., Tarzia, G., Rana, G. L., Calignano, A., Giustino, A., Tattoli, M., Palmery, M., Cuomo, V., & Piomelli, D. (2003). Modulation of anxiety through blockade of anandamide hydrolysis. *Nature Medicine*, *9*(1), 76–81. https://doi.org/10.1038/nm803

Katona, I., & Freund, T. F. (2008). Endocannabinoid signaling as a synaptic circuit breaker in neurological disease. *Nature Medicine*, *14*(9), 923–930. https://doi.org/10.1038/nm.f.1869

Kaufman, M. P., Iwamoto, G. A., Longhurst, J. C., & Mitchell, J. H. (1982). Effects of capsaicin and bradykinin on afferent fibers with ending in skeletal muscle. *Circulation Research*, *50*(1), 133–139. https://doi.org/10.1161/01.RES.50.1.133

Kobayashi, K., Fukuoka, T., Obata, K., Yamanaka, H., Dai, Y., Tokunaga, A., & Noguchi, K. (2005). Distinct expression of TRPM8, TRPA1, and TRPV1 mRNAs in rat primary afferent neurons with aδ/c-fibers and colocalization with trk receptors. *Journal of Comparative Neurology*, *493*(4), 596–606. https://doi.org/10.1002/cne.20794

Kohno, M., Hasegawa, H., Inoue, A., Muraoka, M., Miyazaki, T., Oka, K., & Yasukawa, M. (2006). Identification of N-arachidonylglycine as the endogenous ligand for orphan G-protein-coupled receptor GPR18. *Biochemical and Biophysical Research Communications*, *347*(3), 827–832. https://doi.org/10.1016/j.bbrc.2006.06.175

Kudsi, S. Q., Piccoli, B. C., Ardisson-Araújo, D., & Trevisan, G. (2022). Transcriptional landscape of TRPV1, TRPA1, TRPV4, and TRPM8 channels throughout human tissues. *Life Sciences*, *308*, 120977. https://doi.org/10.1016/j.lfs.2022.120977

Lambert, D. M., Vandevoorde, S., Diependaele, G., Govaerts, S. J., & Robert, A. R. (2001). Anticonvulsant Activity of N-Palmitoylethanolamide, a Putative Endocannabinoid, in Mice. *Epilepsia*, *42*(3), 321–327. https://doi.org/10.1046/j.1528-1157.2001.41499.x

Leggett, J. D., Aspley, S., Beckett, S. R. G., D'Antona, A. M., Kendall, D. A., & Kendall, D. A. (2004). Oleamide is a selective endogenous agonist of rat and human CB1 cannabinoid receptors. *British Journal of Pharmacology*, *141*(2), 253–262. https://doi.org/10.1038/sj.bjp.0705607

Leishman, E., Mackie, K., Luquet, S., & Bradshaw, H. B. (2016). Lipidomics profile of a NAPE-PLD KO mouse provides evidence of a broader role of this enzyme in lipid metabolism in the brain. *Biochimica et Biophysica Acta (BBA) - Molecular and Cell Biology of Lipids*, *1861*(6), 491–500. https://doi.org/10.1016/j.bbalip.2016.03.003

Li, Yitian, Zhou, P., Hu, T., Ren, J., Xu, Y., Qiu, Y., Lu, C., & Li, Yuhang. (2021). NAAA inhibitor F96 attenuates BBB disruption and secondary injury after traumatic brain injury (TBI). *European Journal of Pharmacology*, *912*, 174561. https://doi.org/10.1016/j.ejphar.2021.174561

Lian, J., Casari, I., & Falasca, M. (2022). Modulatory role of the endocannabinoidome in the pathophysiology of the gastrointestinal tract. *Pharmacological Research*, *175*, 106025. https://doi.org/10.1016/j.phrs.2021.106025

Lin, S., Khanolkar, A. D., Fan, P., Goutopoulos, A., Qin, C., Papahadjis, D., & Makriyannis, A. (1998). Novel Analogues of Arachidonylethanolamide (Anandamide): Affinities for the CB1

and CB2 Cannabinoid Receptors and Metabolic Stability. *Journal of Medicinal Chemistry*, *41*(27), 5353–5361. https://doi.org/10.1021/jm970257g

Liu, W. M., Duan, E. K., & Cao, Y. J. (2002). Effects of anandamide on embryo implantation in the mouse. *Life Sciences*, *71*(14), 1623–1632. https://doi.org/10.1016/S0024-3205(02)01928-8

Lo Verme, J., Fu, J., Astarita, G., La Rana, G., Russo, R., Calignano, A., & Piomelli, D. (2005). The Nuclear Receptor Peroxisome Proliferator-Activated Receptor-α Mediates the Anti-Inflammatory Actions of Palmitoylethanolamide. *Molecular Pharmacology*, *67*(1), 15–19. https://doi.org/10.1124/mol.104.006353

Lu, H.-C., & Mackie, K. (2021). Review of the Endocannabinoid System. *Biological Psychiatry. Cognitive Neuroscience and Neuroimaging*, *6*(6), 607–615. https://doi.org/10.1016/j.bpsc.2020.07.016

Lu, V. B., Puhl, H. L., & Ikeda, S. R. (2013). *N*-Arachidonyl Glycine Does Not Activate G Protein–Coupled Receptor 18 Signaling via Canonical Pathways. *Molecular Pharmacology*, *83*(1), 267–282. https://doi.org/10.1124/mol.112.081182

Mannochio-Russo, H., Charron-Lamoureux, V., Faassen, M. van, Lamichhane, S., Nunes, W. D. G., Deleray, V., Ayala, A. V., Tanaka, Y., Patan, A., Vittali, K., Rajkumar, P., Abiead, Y. E., Zhao, H. N., Gomes, P. W. P., Mohanty, I., Lee, C., Sund, A., Sharma, M., Liu, Y., … Dorrestein, P. C. (2025). The microbiome diversifies long- to short-chain fatty acid-derived N-acyl lipids. *Cell*, *188*(15), 4154-4169.e19. https://doi.org/10.1016/j.cell.2025.05.015

Marchioni, C., De Souza, I. D., Acquaro, V. R., De Souza Crippa, J. A., Tumas, V., & Queiroz, M. E. C. (2018). Recent advances in LC-MS/MS methods to determine endocannabinoids in biological samples: Application in neurodegenerative diseases. *Analytica Chimica Acta*, *1044*, 12–28. https://doi.org/10.1016/j.aca.2018.06.016

Martins, D., Tavares, I., & Morgado, C. (2014). “Hotheaded”: The role OF TRPV1 in brain functions. *Neuropharmacology*, *85*, 151–157. https://doi.org/10.1016/j.neuropharm.2014.05.034

Martínez-González, D., Bonilla-Jaime, H., Morales-Otal, A., Henriksen, S. J., Velázquez-Moctezuma, J., & Prospéro-García, O. (2004). Oleamide and anandamide effects on food intake and sexual

behavior of rats. *Neuroscience Letters*, *364*(1), 1–6. https://doi.org/10.1016/j.neulet.2004.03.080

Mathison, R., Ho, W., Pittman, Q. J., Davison, J. S., & Sharkey, K. A. (2004). Effects of cannabinoid receptor-2 activation on accelerated gastrointestinal transit in lipopolysaccharide-treated rats. *British Journal of Pharmacology*, *142*(8), 1247–1254. https://doi.org/10.1038/sj.bjp.0705889

Matsuda, L. A., Lolait, S. J., Brownstein, M. J., Young, A. C., & Bonner, T. I. (1990). Structure of a cannabinoid receptor and functional expression of the cloned cDNA. *Nature*, *346*(6284), 561–564. https://doi.org/10.1038/346561a0

Mátyás, F., Urbán, G. M., Watanabe, M., Mackie, K., Zimmer, A., Freund, T. F., & Katona, I. (2008). Identification of the sites of 2-arachidonoylglycerol synthesis and action imply retrograde endocannabinoid signaling at both GABAergic and glutamatergic synapses in the ventral tegmental area. *Neuropharmacology, Cannabinoid Signaling in the Nervous System*, *54*(1), 95–107. https://doi.org/10.1016/j.neuropharm.2007.05.028

McHugh, D., Hu, S. S., Rimmerman, N., Juknat, A., Vogel, Z., Walker, J. M., & Bradshaw, H. B. (2010). N-arachidonoyl glycine, an abundant endogenous lipid, potently drives directed cellular migration through GPR18, the putative abnormal cannabidiol receptor. *BMC Neuroscience*, *11*(1), 44. https://doi.org/10.1186/1471-2202-11-44

McHugh, D., Page, J., Dunn, E., & Bradshaw, H. B. (2012). Δ9-Tetrahydrocannabinol and N-arachidonyl glycine are full agonists at GPR18 receptors and induce migration in human endometrial HEC-1B cells. *British Journal of Pharmacology*, *165*(8), 2414–2424. https://doi.org/10.1111/j.1476-5381.2011.01497.x

McHugh, D., Wager-Miller, J., Page, J., & Bradshaw, H. B. (2012). siRNA knockdown of GPR18 receptors in BV-2 microglia attenuates N-arachidonoyl glycine-induced cell migration. *Journal of Molecular Signaling*, *7*, 10. https://doi.org/10.1186/1750-2187-7-10

Mock, E. D., Gagestein, B., & van der Stelt, M. (2023). Anandamide and other *N*-acylethanolamines: A class of signaling lipids with therapeutic opportunities. *Progress in Lipid Research*, *89*, 101194. https://doi.org/10.1016/j.plipres.2022.101194

Moon, S.-M., Lee, S. Ah., Hong, J. H., Kim, J.-S., Kim, D. K., & Kim, C. S. (2018). Oleamide suppresses inflammatory responses in LPS-induced RAW264.7 murine macrophages and alleviates paw edema in a carrageenan-induced inflammatory rat model. *International Immunopharmacology*, *56*, 179–185. https://doi.org/10.1016/j.intimp.2018.01.032

Movahed, P., Jönsson, B. A. G., Birnir, B., Wingstrand, J. A., Jørgensen, T. D., Ermund, A., Sterner, O., Zygmunt, P. M., & Högestätt, E. D. (2005). Endogenous Unsaturated C18 N-Acylethanolamines Are Vanilloid Receptor (TRPV1) Agonists. *Journal of Biological Chemistry*, *280*(46), 38496–38504. https://doi.org/10.1074/jbc.M507429200

Munro, S., Thomas, K. L., & Abu-Shaar, M. (1993). Molecular characterization of a peripheral receptor for cannabinoids. *Nature*, *365*(6441), 61–65. https://doi.org/10.1038/365061a0

Musella, A., Fresegna, D., Rizzo, F. R., Gentile, A., Bullitta, S., De Vito, F., Guadalupi, L., Centonze, D., & Mandolesi, G. (2017). A novel crosstalk within the endocannabinoid system controls GABA transmission in the striatum. *Scientific Reports*, *7*(1), 7363. https://doi.org/10.1038/s41598-017-07519-8

Navarrete, C. M., Pérez, M., De Vinuesa, A. G., Collado, J. A., Fiebich, B. L., Calzado, M. A., & Muñoz, E. (2010). Endogenous N-acyl-dopamines induce COX-2 expression in brain endothelial cells by stabilizing mRNA through a p38 dependent pathway. *Biochemical Pharmacology*, *79*(12), 1805–1814. https://doi.org/10.1016/j.bcp.2010.02.014

Navarrete, M., & Araque, A. (2008). Endocannabinoids Mediate Neuron-Astrocyte Communication. *Neuron*, *57*(6), 883–893. https://doi.org/10.1016/j.neuron.2008.01.029

Nguyen, T., Li, J.-X., Thomas, B. F., Wiley, J. L., Kenakin, T. P., & Zhang, Y. (2017). Allosteric Modulation: An Alternate Approach Targeting the Cannabinoid CB1 Receptor. *Medicinal Research Reviews*, *37*(3), 441–474. https://doi.org/10.1002/med.21418

Niu, Z., Zhang, W., Yu, C., Zhang, J., & Wen, Y. (2018). Recent advances in biological sample preparation methods coupled with chromatography, spectrometry and electrochemistry analysis techniques. *TrAC Trends in Analytical Chemistry*, *102*, 123–146. https://doi.org/10.1016/j.trac.2018.02.005

Oh, D. Y., Yoon, J. M., Moon, M. J., Hwang, J.-I., Choe, H., Lee, J. Y., Kim, J. I., Kim, S., Rhim, H., O'Dell, D. K., Walker, J. M., Na, H. S., Lee, M. G., Kwon, H. B., Kim, K., & Seong, J. Y. (2008). Identification of Farnesyl Pyrophosphate and *N*-Arachidonylglycine as Endogenous Ligands for GPR92*. *Journal of Biological Chemistry*, *283*(30), 21054–21064. https://doi.org/10.1074/jbc.M708908200

Osafo, N., Yeboah, O. K., & Antwi, A. O. (2021). Endocannabinoid system and its modulation of brain, gut, joint and skin inflammation. *Molecular Biology Reports*, *48*(4), 3665–3680. https://doi.org/10.1007/s11033-021-06366-1

Overton, H. A., Babbs, A. J., Doel, S. M., Fyfe, M. C. T., Gardner, L. S., Griffin, G., Jackson, H. C., Procter, M. J., Rasamison, C. M., Tang-Christensen, M., Widdowson, P. S., Williams, G. M., & Reynet, C. (2006). Deorphanization of a G protein-coupled receptor for oleoylethanolamide and its use in the discovery of small-molecule hypophagic agents. *Cell Metabolism*, *3*(3), 167–175. https://doi.org/10.1016/j.cmet.2006.02.004

Owsianik, G., Talavera, K., Voets, T., & Nilius, B. (2006). PERMEATION AND SELECTIVITY OF TRP CHANNELS. *Annual Review of Physiology*, *68*(1), 685–717. https://doi.org/10.1146/annurev.physiol.68.040204.101406

Parmar, N., & Ho, W.-S. V. (2010). N-arachidonoyl glycine, an endogenous lipid that acts as a vasorelaxant via nitric oxide and large conductance calcium-activated potassium channels. *British Journal of Pharmacology*, *160*(3), 594–603. https://doi.org/10.1111/j.1476-5381.2009.00622.x

Pisani, V., Moschella, V., Bari, M., Fezza, F., Galati, S., Bernardi, G., Stanzione, P., Pisani, A., & Maccarrone, M. (2010). Dynamic changes of anandamide in the cerebrospinal fluid of Parkinson's disease patients. *Movement Disorders*, *25*(7), 920–924. https://doi.org/10.1002/mds.23014

Przybyla, J. A., & Watts, V. J. (2010). Ligand-Induced Regulation and Localization of Cannabinoid CB1 and Dopamine D2L Receptor Heterodimers. *The Journal of Pharmacology and Experimental Therapeutics*, *332*(3), 710–719. https://doi.org/10.1124/jpet.109.162701

Rodríguez de Fonseca, F., Navarro, M., Gómez, R., Escuredo, L., Nava, F., Fu, J., Murillo-Rodríguez, E., Giuffrida, A., LoVerme, J., Gaetani, S., Kathuria, S., Gall, C., & Piomelli, D. (2001). An anorexic lipid mediator regulated by feeding. *Nature*, *414*(6860), 209–212. https://doi.org/10.1038/35102582

Rodríguez, J. J., Mackie, K., & Pickel, V. M. (2001). Ultrastructural Localization of the CB1 Cannabinoid Receptor in μ-Opioid Receptor Patches of the Rat Caudate Putamen Nucleus. *The Journal of Neuroscience*, *21*(3), 823. https://doi.org/10.1523/JNEUROSCI.21-03-00823.2001

Rossato, M., Ion Popa, F., Ferigo, M., Clari, G., & Foresta, C. (2005). Human Sperm Express Cannabinoid Receptor Cb1, the Activation of Which Inhibits Motility, Acrosome Reaction, and Mitochondrial Function. *The Journal of Clinical Endocrinology & Metabolism*, *90*(2), 984–991. https://doi.org/10.1210/jc.2004-1287

Rozenfeld, R., Bushlin, I., Gomes, I., Tzavaras, N., Gupta, A., Neves, S., Battini, L., Gusella, G. L., Lachmann, A., Ma'ayan, A., Blitzer, R. D., & Devi, L. A. (2012). Receptor Heteromerization Expands the Repertoire of Cannabinoid Signaling in Rodent Neurons. *PLOS ONE*, *7*(1), e29239. https://doi.org/10.1371/journal.pone.0029239

Sancho, R., Macho, A., de La Vega, L., Calzado, M. A., Fiebich, B. L., Appendino, G., & Muñoz, E. (2004). Immunosuppressive Activity of Endovanilloids: N-Arachidonoyl-Dopamine Inhibits Activation of the NF-κB, NFAT, and Activator Protein 1 Signaling Pathways 1. *The Journal of Immunology*, *172*(4), 2341–2351. https://doi.org/10.4049/jimmunol.172.4.2341

Sayd, A., Antón, M., Alén, F., Caso, J. R., Pavón, J., Leza, J. C., Rodríguez de Fonseca, F., García-Bueno, B., & Orio, L. (2015). Systemic Administration of Oleoylethanolamide Protects from Neuroinflammation and Anhedonia Induced by LPS in Rats. *International Journal of Neuropsychopharmacology*, *18*(6), pyu111. https://doi.org/10.1093/ijnp/pyu111

Scuderi, C., Bronzuoli, M. R., Facchinetti, R., Pace, L., Ferraro, L., Broad, K. D., Serviddio, G., Bellanti, F., Palombelli, G., Carpinelli, G., Canese, R., Gaetani, S., Steardo, L., Steardo, L., & Cassano, T. (2018). Ultramicronized palmitoylethanolamide rescues learning and memory impairments in a triple transgenic mouse model of Alzheimer's disease by exerting anti-

inflammatory and neuroprotective effects. *Translational Psychiatry*, *8*(1), 1–19. https://doi.org/10.1038/s41398-017-0076-4

Sharkey, K. A., & Wiley, J. W. (2016). The Role of the Endocannabinoid System in the Brain–Gut Axis. *Gastroenterology*, *151*(2), 252–266. https://doi.org/10.1053/j.gastro.2016.04.015

Shen, B., Yang, G., Lv, M., Wu, Z., Zhang, Y., Cao, Y., Shu, J., Dong, W., Hou, Z., Jing, D., Xu, J., Hou, Y., Zhang, X., Hong, S., & Li, L. (2025). Cannabidiol attenuates methamphetamine-induced oxidative neurotoxicity via regulating transient receptor potential vanilloid type 1. *Phytomedicine*, *145*, 157015. https://doi.org/10.1016/j.phymed.2025.157015

Simard, M., Archambault, A.-S., Lavoie, J.-P. C., Dumais, É., Di Marzo, V., & Flamand, N. (2022). Biosynthesis and metabolism of endocannabinoids and their congeners from the monoacylglycerol and *N*-acyl-ethanolamine families. *Biochemical Pharmacology*, *205*, 115261. https://doi.org/10.1016/j.bcp.2022.115261

Skaper, S. D., Buriani, A., Dal Toso, R., Petrelli, L., Romanello, S., Facci, L., & Leon, A. (1996). The ALIAmide palmitoylethanolamide and cannabinoids, but not anandamide, are protective in a delayed postglutamate paradigm of excitotoxic death in cerebellar granule neurons. *Proceedings of the National Academy of Sciences*, *93*(9), 3984–3989. https://doi.org/10.1073/pnas.93.9.3984

Spicarova, D., & Palecek, J. (2009). The Role of The TRPV1 Endogenous Agonist N-Oleoyldopamine in Modulation of Nociceptive Signaling at the Spinal Cord Level. *Journal of Neurophysiology*, *102*(1), 234–243. https://doi.org/10.1152/jn.00024.2009

Staiano, R. I., Loffredo, S., Borriello, F., Iannotti, F. A., Piscitelli, F., Orlando, P., Secondo, A., Granata, F., Lepore, M. T., Fiorelli, A., Varricchi, G., Santini, M., Triggiani, M., Di Marzo, V., & Marone, G. (2016). Human lung-resident macrophages express CB1 and CB2 receptors whose activation inhibits the release of angiogenic and lymphangiogenic factors. *Journal of Leukocyte Biology*, *99*(4), 531–540. https://doi.org/10.1189/jlb.3HI1214-584R

Stella, N. (2010). Cannabinoid and cannabinoid-like receptors in microglia, astrocytes, and astrocytomas. *Glia*, *58*(9), 1017–1030. https://doi.org/10.1002/glia.20983

Storr, M. A., & Sharkey, K. A. (2007). The endocannabinoid system and gut–brain signalling. *Current Opinion in Pharmacology*, *7*(6), 575–582. https://doi.org/10.1016/j.coph.2007.08.008

Sun, Y., Alexander, S. P. H., Garle, M. J., Gibson, C. L., Hewitt, K., Murphy, S. P., Kendall, D. A., & Bennett, A. J. (2007). Cannabinoid activation of PPARα; a novel neuroprotective mechanism. *British Journal of Pharmacology*, *152*(5), 734. https://doi.org/10.1038/sj.bjp.0707478

Thomas, E. A., Carson, M. J., Neal, M. J., & Sutcliffe, J. G. (1997). Unique allosteric regulation of 5-hydroxytryptamine receptor-mediated signal transduction by oleamide. *Proceedings of the National Academy of Sciences*, *94*(25), 14115–14119. https://doi.org/10.1073/pnas.94.25.14115

Tominaga, M., Caterina, M. J., Malmberg, A. B., Rosen, T. A., Gilbert, H., Skinner, K., Raumann, B. E., Basbaum, A. I., & Julius, D. (1998). The Cloned Capsaicin Receptor Integrates Multiple Pain-Producing Stimuli. *Neuron*, *21*(3), 531–543. https://doi.org/10.1016/S0896-6273(00)80564-4

Tsuboi, K., Uyama, T., Okamoto, Y., & Ueda, N. (2018). Endocannabinoids and related N-acylethanolamines: Biological activities and metabolism. *Inflammation and Regeneration*, *38*(1), 28. https://doi.org/10.1186/s41232-018-0086-5

Turu, G., & Hunyady, L. (2010). *Signal transduction of the CB1 cannabinoid receptor*. https://doi.org/10.1677/JME-08-0190

Ueda, N., Yamanaka, K., & Yamamoto, S. (2001). Purification and Characterization of an Acid Amidase Selective for *N*-Palmitoylethanolamine, a Putative Endogenous Anti-inflammatory Substance*. *Journal of Biological Chemistry*, *276*(38), 35552–35557. https://doi.org/10.1074/jbc.M106261200

Walker, J. M., Huang, S. M., Strangman, N. M., Tsou, K., & Sañudo-Peña, M. C. (1999). Pain modulation by release of the endogenous cannabinoid anandamide. *Proceedings of the National Academy of Sciences*, *96*(21), 12198–12203. https://doi.org/10.1073/pnas.96.21.12198

Waluk, D. P., Battistini, M. R., Dempsey, D. R., Farrell, E. K., Jeffries, K. A., Mitchell, P., Hernandez, L. W., McBride, J. C., Merkler, D. J., & Hunt, M. C. (2014). Mammalian Fatty

Acid Amides of the Brain and CNS. In *Omega-3 Fatty Acids in Brain and Neurological Health* (pp. 87–107). Elsevier. https://doi.org/10.1016/B978-0-12-410527-0.00009-0

Wei, B. Q., Mikkelsen, T. S., McKinney, M. K., Lander, E. S., & Cravatt, B. F. (2006). A Second Fatty Acid Amide Hydrolase with Variable Distribution among Placental Mammals*. *Journal of Biological Chemistry*, *281*(48), 36569–36578. https://doi.org/10.1074/jbc.M606646200

Williams, C. M., & Kirkham, T. C. (1999). Anandamide induces overeating: Mediation by central cannabinoid (CB1) receptors. *Psychopharmacology*, *143*(3), 315–317. https://doi.org/10.1007/s002130050953

Wright, K., Rooney, N., Feeney, M., Tate, J., Robertson, D., Welham, M., & Ward, S. (2005). Differential Expression of Cannabinoid Receptors in the Human Colon: Cannabinoids Promote Epithelial Wound Healing. *Gastroenterology*, *129*(2), 437–453. https://doi.org/10.1053/j.gastro.2005.05.026

Yu, S., Levi, L., Casadesus, G., Kunos, G., & Noy, N. (2014). Fatty Acid-binding Protein 5 (FABP5) Regulates Cognitive Function Both by Decreasing Anandamide Levels and by Activating the Nuclear Receptor Peroxisome Proliferator-activated Receptor β/δ (PPARβ/δ) in the Brain*♦. *Journal of Biological Chemistry*, *289*(18), 12748–12758. https://doi.org/10.1074/jbc.M114.559062

Zoerner, A. A., Gutzki, F.-M., Batkai, S., May, M., Rakers, C., Engeli, S., Jordan, J., & Tsikas, D. (2011). Quantification of endocannabinoids in biological systems by chromatography and mass spectrometry: A comprehensive review from an analytical and biological perspective. *Biochimica et Biophysica Acta (BBA) - Molecular and Cell Biology of Lipids, Lipidomics and Imaging Mass Spectrometry*, *1811*(11), 706–723. https://doi.org/10.1016/j.bbalip.2011.08.004

Zygmunt, P. M., Petersson, J., Andersson, D. A., Chuang, H., Sørgård, M., Di Marzo, V., Julius, D., & Högestätt, E. D. (1999). Vanilloid receptors on sensory nerves mediate the vasodilator action of anandamide. *Nature*, *400*(6743), 452–457. https://doi.org/10.1038/22761

Appendices

Table A1: Targeted mass spectrometry parameters for N-acyl amides

N-acyl amide	Precursor ion *(m/z)*	Fragment ion *(m/z)*	Retention time (min)	Collision energy (V)
AEA-d8	356.33990	63.0656	13.75	25
aLEA-d4	326.2992	66.0849	13.20	25
Amylamine-C13:1	282.27914	88.1119	13.67	25
Amylamine-C21:0	396.41999	130.1218	15.3	35
Arg-C4:0	245.16082	158.0924	0.95	35
Arg-C5:0	259.17647	158.0924	1.59	35
Arg-C8:0	301.22342	116.0700	5.1	35
Arg-C16:0	413.34862	158.0925	11.41	35
Arg-C18:0	441.37992	158.0921	12.29	35
Arg-C18:1	439.36427	158.0925	11.83	35
Arg-C18:2	437.34862	158.0921	11.37	35
GABA-C17:0	356.31592	104.0703	14.25	25
GABA-C20:0	398.36287	104.0706	14.77	35
His-C5:0	240.13427	110.0711	1.31	25
His-C7:0	268.16557	110.0700	3.53	25
His-C16:0	394.30642	110.0710	11.95	25
His-C18:1	420.32207	110.0714	12.38	35
Histamine-C4:0	182.12879	95.0599	0.73	25
Histamine-C5:0	196.14444	112.0869	1.21	25
Histamine-C6:0	210.16009	112.0870	2.08	25
Histamine-C16:0	350.31659	112.0871	10.97	25
Histamine-C18:0	378.34789	112.0946	11.84	35
Histamine-C18:1	376.33224	112.0869	11.37	35
Leu-C17:1	382.33157	132.1015	14.35	25
Leu-C18:1	396.34722	132.1018	14.53	25
Leu-C19:0	412.37852	132.1000	14.80	25
Lys-C16:0_1	385.34247	147.1100	11.35	35
Lys-C16:0_2	385.34247	147.1100	13.11	35

N-acyl amide	Precursor ion *(m/z)*	Fragment ion *(m/z)*	Retention time (min)	Collision energy (V)
Lys-C16:1_1	383.32682	147.1100	10.76	35
Lys-C16:1_2	383.32682	147.1100	12.56	35
Lys-C18:0_1	413.37377	147.1100	12.12	35
Lys-C18:0_2	413.37377	147.1100	13.88	35
Lys-C18:1_1	411.35812	147.1122	11.80	35
Lys-C18:1_2	411.35812	147.1126	13.48	35
OEA-d4	330.33050	66.0849	14.08	25
Ornithine-C20:1_1	425.37377	116.0706	12.60	35
Ornithine-C20:1_2	425.37377	116.0706	14.03	35
Phe-C16:0	404.31592	149.0598	14.52	25
Phe-C18:0	432.34722	149.0261	14.74	25
Phe-C18:1	430.33157	149.0599	14.55	25
Putrecine-C15:0	313.32134	296.2941	10.51	25
Putrecine-C18:2	351.33699	334.3104	10.94	35
SEA-d3	331.33980	62.0598	14.35	25
Ser-C15:0	330.26389	88.0388	13.74	25
Ser-C16:0	344.27954	60.0443	14.08	25
Thr-C18:0	386.32649	74.0596	14.60	25
Thr-C22:3_1	436.34214	120.0700	14.10	25
Thr-C22:3_2	436.34214	120.0700	14.28	25
Tyr-C16:0	420.31084	136.0760	14.00	25
Tyr-C17:0	434.32649	136.0759	14.20	25
Tyr-C18:0	448.34214	136.0750	14.38	25
Val-C18:0	384.34722	86.0960	14.43	25

Table A2: sMRM N-acyl amide detection in pooled QC samples

Detected		Undetected
Arg-C16:0	Lys-C16:0_1	Arg-C18:2
Arg-C18:0	Lys-C16:0_2	Histamine-C6:0
Arg-C18:1	Lys-C18:0_1	His-C7:0
Arg-C4:0	Lys-C18:0_2	Amylamine-C13:1
Arg-C5:0	Lys-C18:1_1	Amylamine-C21:0
Arg-C8:0	Phe-C16:0	Putrescine-C15:0
GABA-C17:0	Phe-C18:0	GABA-C20:0
His-C16:0	Phe-C18:1	Leu-C19:0
His-C18:1	Putrescine-C18:2	Lys-C16:1_1
His-C5:0	Ser-C15:0	Lys-C16:1_2
Histamine-C16:0	Ser-C16:0	Lys-C18:1_2
Histamine-C18:0	Thr-C18:0	Thr-C22:3_1
Histamine-C18:1	Tyr-C16:0	Thr-C22:3_2
Histamine-C4:0	Tyr-C17:0	Ornithine-20:1_1
Histamine-C5:0	Tyr-C18:0	Ornithine-20:1_2
Leu-C17:1	Val-C18:0	
Leu-C18:1		

Figure A1: Fragmentation profiles of histamine-C5:0 and arginine-C18:0

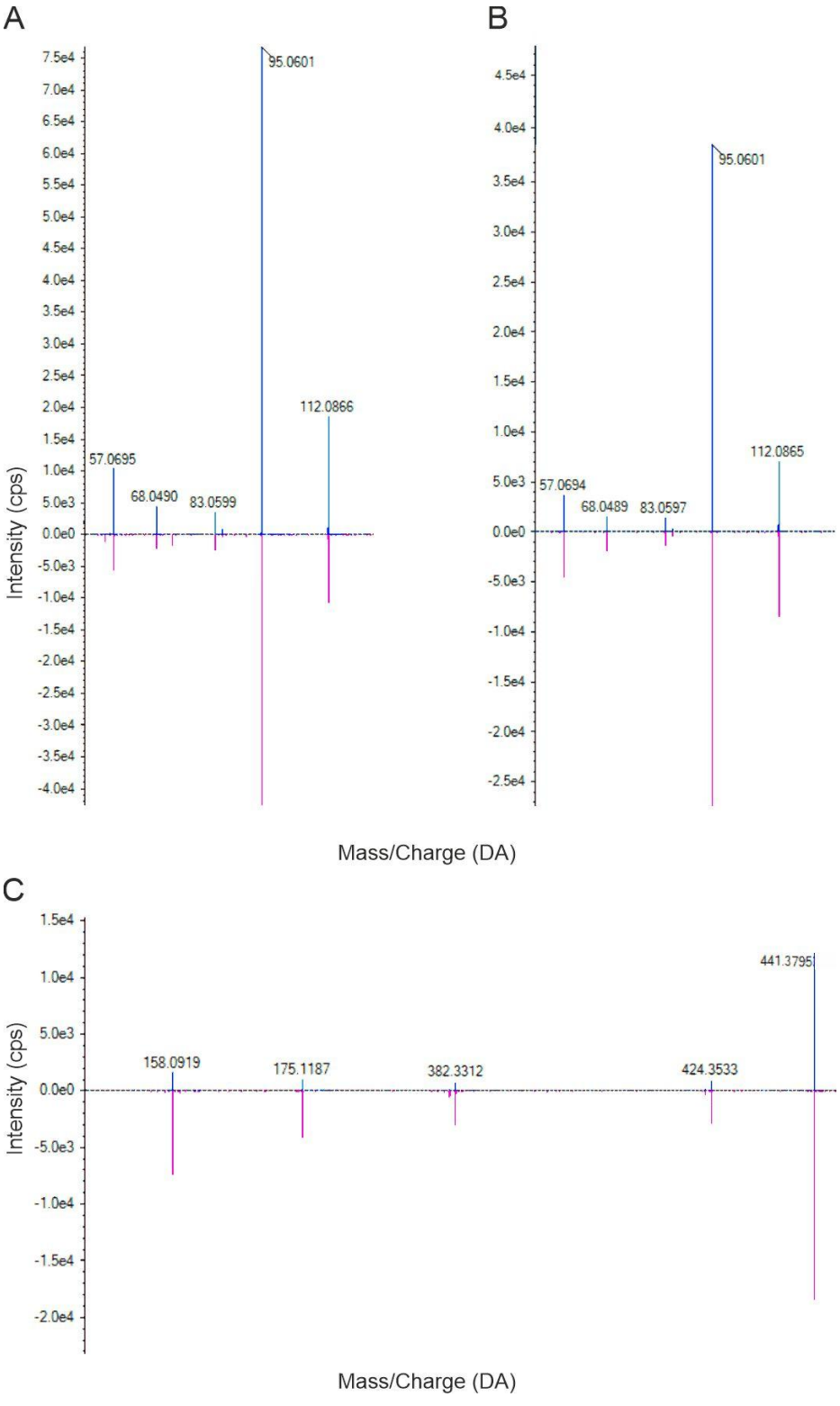

Figure A1. Fragmentation profiles of histamine-C5:0 and Arg-C18:0 compared between in-house (blue) and standard mixture (pink) obtained with positive-ion ESI-MS/MS. A) Fragmentation profile of histamine-C5:0 precursor ion 196.1 *m/z* at 0.563 min (in-house) and 0.552 min (standard mixture). B) Fragmentation profile of histamine-C5:0 precursor ion 196.1 *m/z* at 1.247 min (in-house) and 1.268 min (standard mixture). C) Fragmentation profile of Arg-C18:0 precursor ion 441.3795 *m/z* at 12.235 min (in-house) and 12.280 min (standard mixture). The CE used for the fragmentation was 35V.

Figure A2: 2D NMR correlation spectroscopy of histamine-C5:0

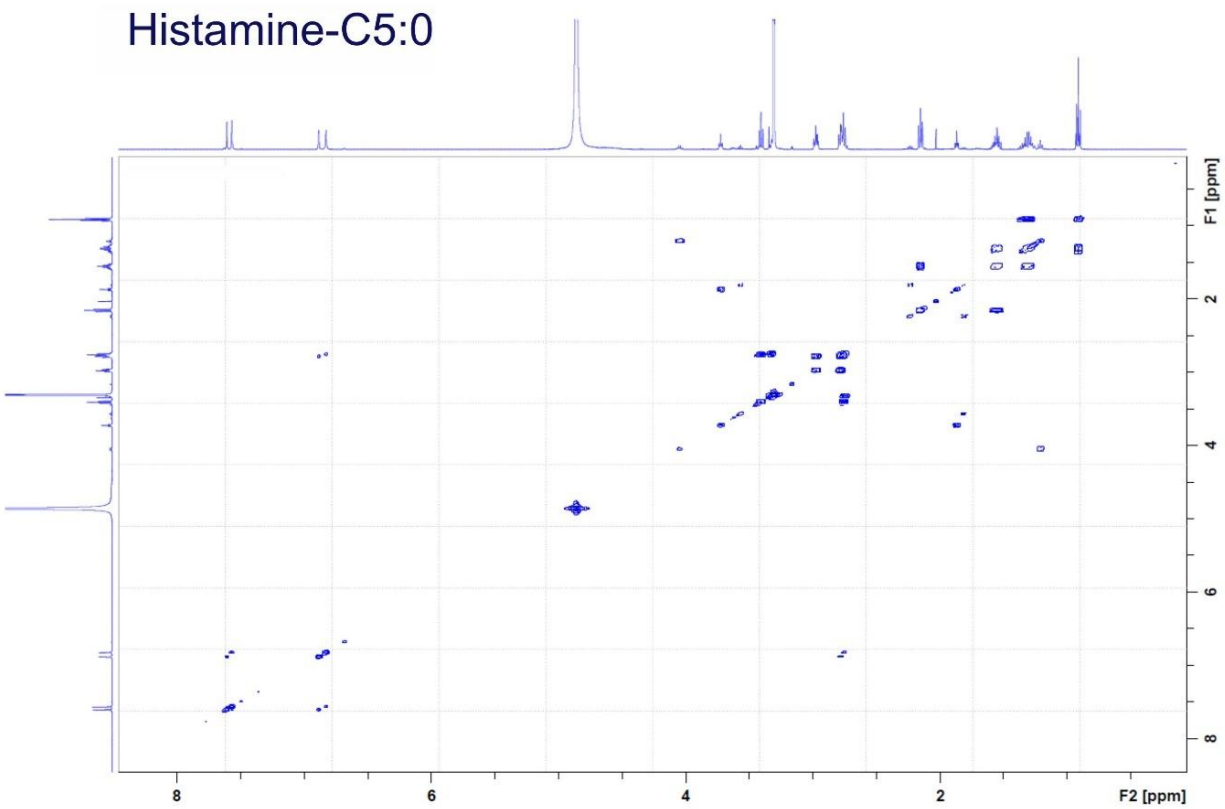

Figure A2. 2D NMR correlation spectroscopy of histamine-C5:0 in methanol-d4 recorded at 500 MHz.

Figure A3: 2D NMR correlation spectroscopy of arginine-C18:0

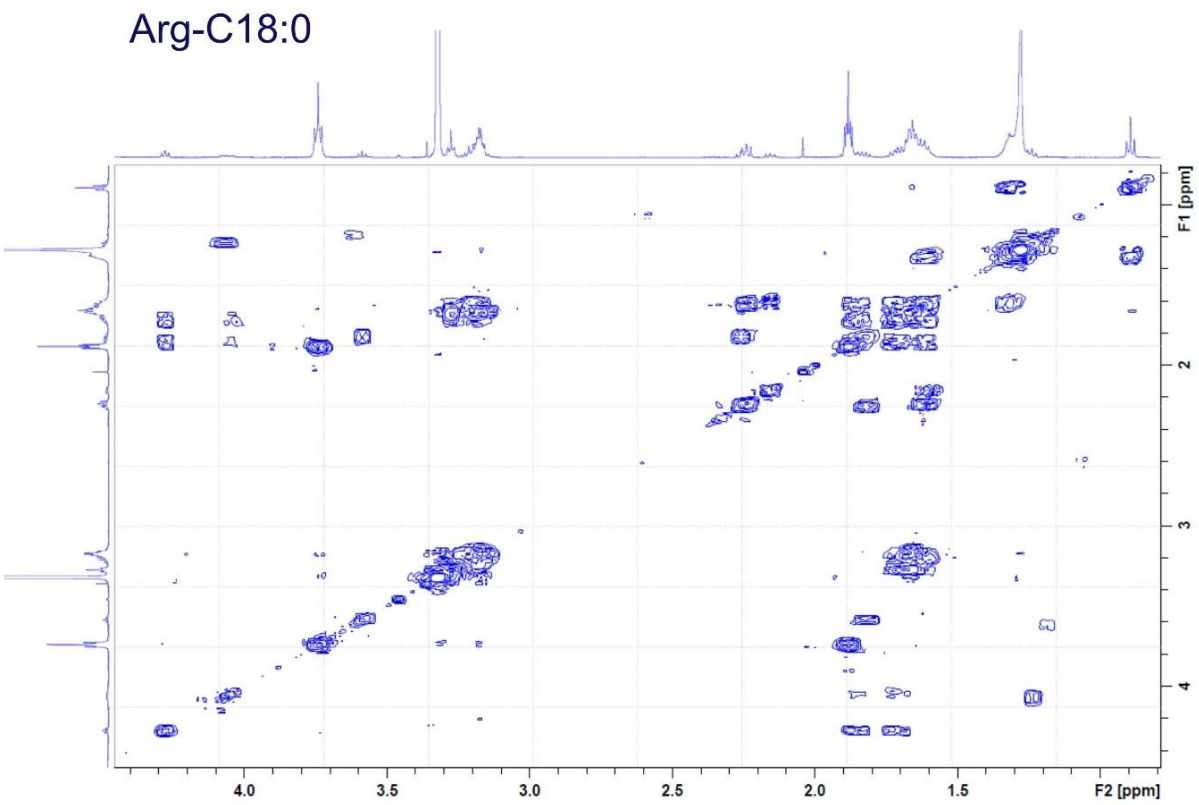

Figure A3. 2D NMR correlation spectroscopy of Arg-C18:0 in methanol-d4 and chloroform-d recorded at 500 MHz.

Figure A4: Arginine-C4:0 peak splitting

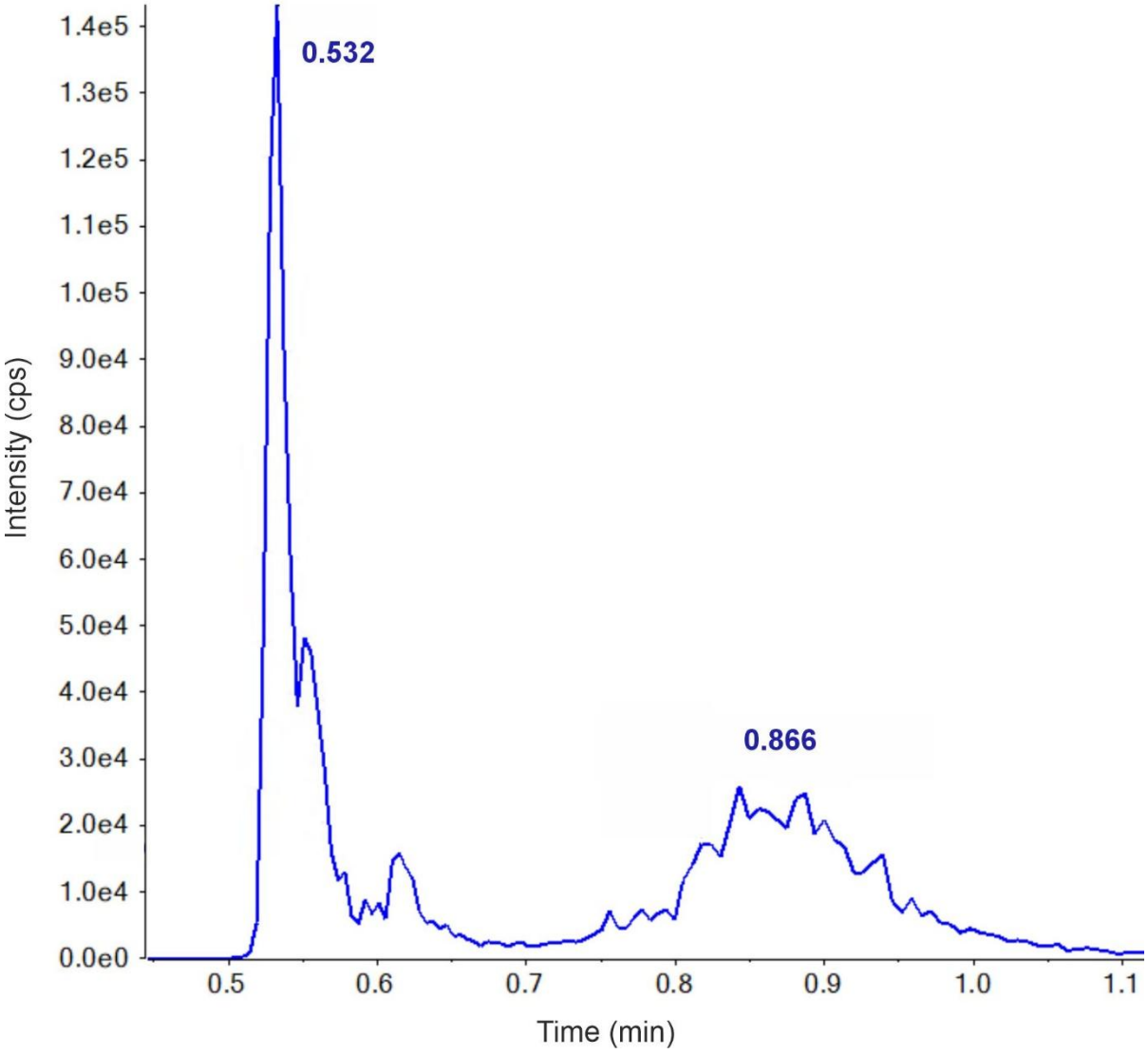

Figure A4. XIC of Dorrestein standard mixture Arg-C4:0 at *m/z* 245.16082 obtained with sMRM LC-MS/MS analysis. Reverse-phase C18 column (Phenomenex Kinetex 1.7 µm 100 x 2.1 mm XB-C18 100 Å column with Phenomenex SecurityGuard ULTRA Cartridge pre-column) was used in UPLC separation. Precursor ion mass errors were within ± 1.0 ppm and fragment mass errors within ± 5.0 ppm for both of the peaks.